Mestrado Integrado em Engenharia Química

Utilization of New Adsorbent materials for CO_2 Capture

Master's Thesis

by

Maria Francisca Couto Moreno Mora Morais

Developed in the context of course Dissertation

conducted in

SINTEF

Supervisor in FEUP: **Professor Adélio Mendes**

Supervisor in SINTEF: **Dr. Eng. Carlos Grande**

Departamento de Engenharia Química

July, 2014

Acknowledgment

Research Council of Norway through the RENERGI program by the project Novel Materials for Utilization of Natural Gas and Hydrogen (grant 190980/S60) is gratefully acknowledged.

I am extremely grateful to Carlos Adolfo Grande and Richard Blom for making this research internship possible at SINTEF and to Adélio Mendes that made the proposal and shared so much knowledge.

I would like to thank Jasmina Hafizovic Cavka for all the support in MAMS' project and also to Bjørnar Arstad for the support in the SBSSA's project.

I am also very grateful to Aud I. Spjelkavik, Anna Maria Lind, Kari Anne Andreassen, Anne Andersen, Marit Synnøve Sæverud Stange and Yngve Larring for sharing so much time and knowledge with me and for being available when needed with so much patience.

In order to make this research work and to complete my master degree in chemical engineering, it was very important the tremendous support from my family, boyfriend and friends that never let me quit, giving me all the strength every time I needed.

Abstract

This project was developed at SINTEF, Oslo (Norway) in the Sorbent Technologies department framed within the Novel Materials for Utilization of Natural Gas and Hydrogen project funded by the Research Council of Norway.

Nowadays, CO_2 emissions to the atmosphere are of great concern. Carbon-capture and storage (CCS) is been considered as an intermediate solution until technologies for generating energy from renewable sources are fully available. Following, the objective of this thesis is the development of two different porous adsorbents to selectively separate carbon dioxide from different streams. The synthetized materials were a mesh-adjustable molecular sieve (MAMS) [1] and a sodium-based sorbent supported in alumina (SBSSA), material which had minimal information about preparation disclosed. All the synthetized samples were fully characterized.

Some difficulties were encountered in reproducing the selected MAMS samples with the same reported performance and in larger production amounts (0.2 g/batch). MAMS project ended with these results.

The SBSSA production method can be improved, however, after some breakthrough measurements it was noticed that the samples are able to capture some CO_2 but this process is enhanced by the H_2O presence due to the carbonate/bicarbonate cycle. Still, it was noticed that the samples capacity for CO_2 is inversely proportional to the sodium carbonate weight in the sample. Nonetheless, the water working capacity increases according to N40 > N10 > N20. For a better understanding of both materials, it would be also necessary to further characterize the samples. As a consequence of this project, the Sorbent Technologies department on SINTEF will continue the research on SBSSA.

Declaration

I declare, on my word of honour, that this is an original work and that all non-original contributions were properly referenced identifying the source.

Signature and date

Index

Figures Index

Tables Index

Notation and Glossary

A	Constant (77.345) associated to equation 4-1	
A_m	Adsorption cross section area for an adsorbed N_2 molecule (0.162 nm^2)	nm^2
B	Constant (0.0057) associated to equation 4-1	
C	Dimensionless constant that is related to the enthalpy of adsorption of the adsorbate gas on the powder sample (equation 3-1)	
$C_{0,\,i}$	Molar concentration of each gas (i) at the entrance of the column	mol/L
C_E	Molar concentration at the entrance of the column	mol/L
C_i	Concentration of each gas (i) at each recorded time from the MS.	mol/L
D	Mesh size at temperature T (equation 2-1)	Å
D_0	Mesh size at zero Kelvin	Å
E	Constant (7235) associated to equation 4-1	
F	Constant (8.2) associated to equation 4-1	
$Intensity_i$	Signal read on the MS	
m_{ads}	Adsorbent weight used in the column	g
m_{Al2O3}	Alumina weight	g
$m_{H2(bbdc)}$	5-tert-butyl-1,3-benzenedicarboxylic acid (H_2(bbdc)) weight	g
m_{Na2CO3}	Sodium carbonate weight	g
$m_{product}$	Product weight	g
M_v	Molar ideal volume for N_2 (22.414 L/mol)	L/mol
N_A	Avogadro's number ($6.022x10^{23}$ mol^{-1})	mol^{-1}
P	Partial vapour pressure of adsorbate gas in equilibrium with the surface at 77 K	Pa
P_0	Saturated pressure of adsorbate gas	Pa
P_E	Pressure at the entrance of the column	Pa
P_{WS}	Saturation pressure of water vapour in air vapour mixture	Pa
Q	Volumetric flow rate	mL/min

q_{total}	Total capacity of the material	mol/kg
R	Constant of ideal gases	m^3.Pa/(mol.K)
S_{BET}	BET surface area	m^2/g
T	temperature	K
T_{cryst}	Crystallization temperature	K
t_{cryst}	Crystallization time	min
T_E	Temperature at the entrance of the column	K
t_{est}	Stoichiometric time	min
T_{mix}	Mixing temperature	K
V_a	Volume of gas adsorbed at standard temperature and pressure (STP – 273.15 K and $1.013x10^5$ Pa)	mL
$V_{Et\ Glicol}$	Etilene glycol volume	mL
V_{H2O}	Distilled water volume	mL
V_m	Volume of gas adsorbed at STP to produce an apparent monolayer on the sample surface	mL
$y_{0,\ i}$	Feed percentage of each gas (i) at the entrance of the column	
y_i	Vapour fraction of each gas on the breakthrough curve measurement	
$\eta_{H2(bbdc)}$	MAMS sample yield based on the 5-tert-butyl-1,3-benzenedicarboxylic acid (H_2(bbdc))	%
α	Constant associated to equation 2-1	

Acronyms list

BET	Brunauer, Emmett and Teller
BSE	Backscatter Electrons
CBS	Circular Backscatter Detector
EDS	Energy Disperse X-ray Spectroscopy
ETD	Everhart-Thornley Detector
GHG	Greenhouse gases
ICDD	International Centre of Diffraction Data
IEA	International Energy Agency

MAMS	Mesh-Adjustable Molecular Sieve
MS	Mass Spectrometer
SBSSA	Sodium-Based Sorbent Supported in Alumina
SE	Secondary Electrons
SEM	Scanning Electron Microscopy
TGA	Thermogravimetric Analysis
XRD	X-ray Diffraction

1 Introduction

It has been already proven that the global warming effect is caused by the large emission of greenhouse gases (GHG) to the atmosphere. From the GHG, carbon dioxide is the most abundant and thus, strategies to avoid its emissions represent one of the most important challenges of mankind.

However, controlling emissions of CO_2 is not an easy task. The sources and operating conditions (temperature, pressure, other gases, etc.) of the streams emitting carbon dioxide are so diversified that almost any technology can find a niche market in this arena.

In this sense, the objective of this thesis has been focused in the development of two very different porous materials aiming to separate carbon dioxide from very different streams.

The first material termed as MAMS (mesh-adjustable molecular sieve) [1] has been synthesized with the aim of removing carbon dioxide from other gases at low temperature. The material has been reported to have unique features of separating molecules at cryogenic temperatures. In that sense, MAMS can be used in the selective removal of carbon dioxide in the natural gas industry, particularly when the final product is liquefied natural gas (LNG).

The second material, carbonate salts dispersed in alumina matrices, aims to capture carbon dioxide at milder temperatures (~70 °C) which is closer to the temperature of the flue gases emitted in power stations (90 °C in natural gas combined cycles power plants and 110 °C in coal-fired power plants). Regeneration in this case is done with heat at higher temperatures that is also available in the power plant, at the expense of less energy generation (negative penalty).

In this sense, the thesis tackles two major sources of carbon dioxide emission: upgrading of natural gas, particularly interesting to Norway, and decarbonizing energy production which is a more global problem.

1.1. Project Presentation

The most important part of this work is related to the synthesis of MAMS metal-organic framework and carbonate salts dispersed in alumina. None of these materials were previously prepared in the Sorbent Technologies department so there was no experience in their synthesis. For this reason, it was known from the beginning that the contents of the thesis were highly depending on the success of synthesis where minimal information about

preparation is disclosed. In that sense, the major objectives of the thesis were to develop the synthesis, characterization and utilization of two different porous materials.

1.2. Company Presentation

The SINTEF group is the largest independent non-commercial research organization in Scandinavia and one of the largest in Europe with over 2000 employees. SINTEF carries out contract research for the industrial and public sectors in Norway and overseas. SINTEF vision is "Technology for a better society". The SINTEF group is divided in eight different brands, from which SINTEF Materials and Chemistry is the largest one with approx. 450 employees.

The thesis was developed within the Department of Sorbent Technologies in the sector of Sustainable Energy Technologies of Materials and Chemistry. The department has around 15 employees having "cradle-to-grave" capabilities in synthesis, characterization, formulation and utilization of solids for different processes (including reactor and process modelling and design).

1.3. Contributes of work

During this internship, some difficulties were encountered on the BELPREP-vacII equipment operation. This is a gas/vapour adsorption pre-treatment instrument that contains the Micro-controller X – PXR3 as a temperature controller. This temperature controller was blocked precluding the heating rate option during the particles activation. Thus, this equipment was fixed enabling the heating rate control.

The TGA equipment used, SETARAM TGA92-16.18, had some problems on the temperature measurements due to its large distance to the sample. Then, it was made a new thermocouple that could be closer to the sample in order to obtain better results on all the samples measurements.

The system for the breakthrough curve measurements was also modified for these experiences in order to obtain signal measurements from the outlet of one column instead of the sum of two columns (R and D as represented in Figure 3-5 and Figure 3-6).

1.4. Organization of the thesis

Chapter 2 starts to appoint some types of solid sorbent to capture and storage carbon dioxide (CCS). On this chapter it is briefly explained MOFs' concept as an introduction to the promising material – MAMS, and also sodium-based sorbent concept.

Chapter 3 describes the materials synthesis as well as the methods used to characterize the samples such as X-ray diffraction (XRD), thermogravimetric analysis (TGA), scanning electron microscopy (SEM) and surface area, isotherm and breakthrough measurements.

Chapter 4 presents and discusses the experimental results obtained as well as the calculations performed for materials characterization.

Chapter 5 concludes all the work realized on this thesis aiming to answer the initial goals.

2 State of the art

Nowadays, there are solid adsorbent materials capable of adsorbing carbon dioxide such as zeolites, mesoporous materials, activated carbon, metal organic frameworks (MOFs), carbonates, etc.

The goal for the best carbon capture and storage (CCS) sorbent selection implies high CO_2 capacity and selectivity, fast adsorption and desorption kinetics, good mechanical properties, high hydrothermal and chemical stability and low cost of synthesis [2].

Metal-Organic Frameworks

MOFs materials have a large surface area and have potential for being employed in numerous applications such as adsorption, gas storage, separation, drug delivery, crystallography and catalysis. However the major disadvantage is in the cost of synthesis.

MOFs structure, as represented in Figure 2-1 [4] is formed by nodes on the lattices made of metal elements which are connected by organic molecules. MOFs' pores are intended to store gases and the framework to channel the gas sorption, thus defining the mesh size for the gas entrance. MOFs' pore shape and size can be adjusted through appropriate selection of metal nodes and organic ligands in order to achieve the desirable material properties [3].

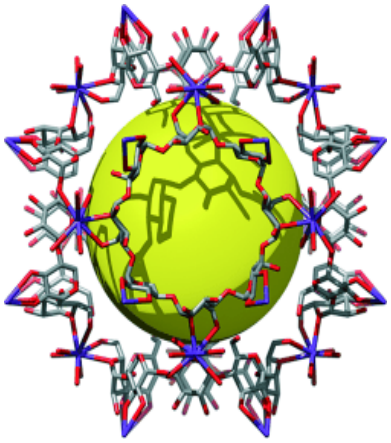

Figure 2-1 - Metal Orgnanic Framework scheme (extracted from [4])

MAMS – Mesh Adjustable Molecular Sieve, is a MOF compound which one of its major advantages is that it has been reported that the pore size can be tuned with the operation temperature. Shengqian Ma et al. [1], reported an innovative MAMS-1 that has a graphitic MOF structure made with nickel as the metal element (nickel nitrate hexahydrate as the reagent that after reaction forms a metal ions/clusters) and 5-tert-butyl-1,3-benzenedicarboxylic acid (H_2(bbcd)) as the organic molecule. This organic molecule is an amphiphilic ligand, i.e., it has hydrophilic and hydrophobic ends, in which the hydrophilic one is functionalized. The functionalized hydrophilic end is the one that attaches the metal ions/clusters by covalent bonds thereby creating continuous 2D layer. Then, two layers will sandwich the metal elements constructing a trilayer, where are located the channels for the gas to pass. Two trilayers are then connected by Van der Waals interactions where the chambers are located for gas storing, as represented in Figure 2-2.

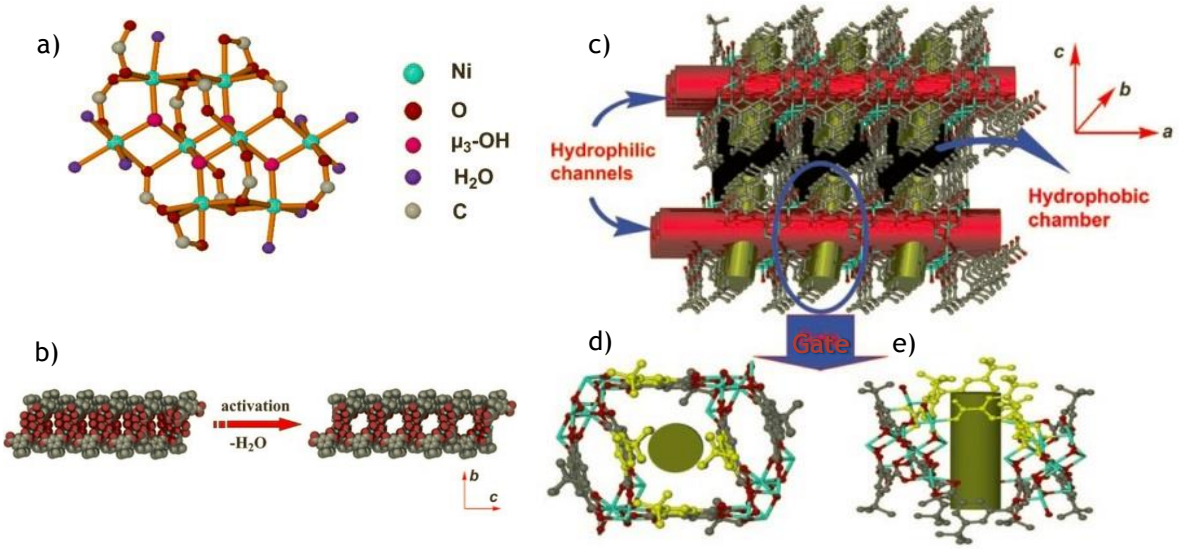

Figure 2-2 - Crystal structure of MAMS-1. a) Structure of the nickel cluster. b) Structure of solvated and desolvated trilayers. c) Two trilayer displays hydrophilic channels along the a axis forming hydrophobic chambers. d) Top and e) side views of bbdc pairs (extracted from [1])

However, the hydrophobic chamber can only be accessed after activation that implies dehydration at 200 °C under vacuum, i.e., it is necessary to remove the water molecules that are occupying the channels.

The production of MAMS-1 is conducted by a solvothermal reaction between the organic and metal compounds, that are 5-tert-butyl-1,3-benzenedicarboxylic acid (H_2(bbdc)) and nickel nitrate hexahydrate ($Ni(NO_3)_2 \cdot 6H_2O$) respectively, in a Teflon-lined covered by a autoclave, in a programmable oven at 210 °C for 24h with a heating rate of 2 °C/min.

In order to define the gate opening of the material with the temperature, Shengqian MA et al. [1], measured some isotherms with different gases at variable temperatures. Considering the different gas molecules size and the MAMS selectivity shown in their isotherms results, they reported an experimental linear equation relating mesh size with temperature (Equation 2-1):

$$D = D_0 + \alpha T \tag{2-1}$$

Where D and D_0 correspond to the mesh size at temperature T (in Kelvin) and at zero Kelvin, respectively; α is a constant. Adjusting D_0 and α they expected to result in some MAMS which might be omnipotent for gas separation at near-ambient temperatures.

The MAMS-1 is expected to have a mesh range between 2.9-5 Å adjustable with the temperature range of 77 K to 300 K.

Sodium-based sorbent

Carbonate minerals are natural materials present in earth containing the carbonate ion CO_3^{2-}.

The principles of the carbon dioxide capture using alkali-based sorbent process lies in the reversible reaction between the carbonate and bicarbonate on a carbon dioxide and water environment.

One possible alkali-based sorbent is sodium carbonate and the carbonate/bicarbonate cycle is represented by the following reactions [5],[6]:

$$Na_2CO_3(s) + CO_2(g) + H_2O(g) \rightarrow 2NaHCO_3(s) \qquad \Delta H_r^o = -135\,kJ/mol\,Na_2CO_3 \tag{2-2}$$

$$2NaHCO_3(s) \rightarrow Na_2CO_3(s) + CO_2(g) + H_2O(g) \tag{2-3}$$

This regenerable sorbent is able to remove the carbon dioxide from a stream at ambient pressure as shown in equation 2-2. The regeneration produces just water and carbon dioxide, as represented in equation 2-3. Posteriorly the water can be removed by condensation producing a pure stream of carbon dioxide ready to be used or to be sequestered [6].

However, there are some possible secondary reactions at equation 2-2 conditions [5]:

$$Na_2CO_3(s) + H_2O(g) \rightleftharpoons Na_2CO_3 \cdot H_2O(s) \tag{2-4}$$

$$Na_2CO_3(s) + \frac{1}{3}CO_2(g) + \frac{5}{3}H_2O(g) \rightleftharpoons \frac{2}{3}Na_2CO_3 \cdot NaHCO_3 \cdot 2H_2O(s) \tag{2-5}$$

$$Na_2CO_3(s) + \frac{3}{5}CO_2(g) + \frac{3}{5}H_2O(g) \rightleftharpoons \frac{2}{5}Na_2CO_3 \cdot 3NaHCO_3(s) \tag{2-6}$$

As reported, the reactions 2-2 and 2-3 happen in the temperature range of 60-70 °C and 120-200 °C respectively [7]. Nonetheless, on the IEA's report, it was recommended to disperse the sodium carbonate on alumina in order to provide attrition resistance, thereby increasing the carbonate performance. They also reported that "supported sorbents should combine attrition resistance inherent to support material and reactivity of carbonate material".

3 Materials and Methods

In this experimental work, it was produced two different solid sorbents: mesh-adjustable molecular sieves and sodium-based sorbent supported in alumina. These materials were submitted to some characterization tests in order to define their structure, distribution and to be tested their performance.

3.1. Materials

The solid sorbents materials: Mesh-Adjustable Molecular Sieves (MAMS) and Sodium-based sorbent supported in alumina (SBSSA), were experimentally produced. For MAMS production it was followed a reported recipe [1] and some process variables were tested in order to analyse its effect on the product features. For SBSSA production there was not found any recipe, thus it was produced by assumptions, considering the desired product features.

3.1.1. MAMS

The following procedure has been used to produce MAMS [1]. Dissolve the nickel nitrate hexahydrate ($Ni(NO_3)_2 \cdot 6H_2O$) and the 5-tert-butyl-1,3-benzenedicarboxylic acid (H_2(bbdc)) in water and ethylene glycol (4:1 v/v), in this order, with the magnetic stir bar in a magnetic stirrer. Add the nickel solution to the organic solution with constant magnetic stirring. Place the solution in a teflon container and sealed in an autoclave. After, put the autoclave in a programmable oven with a heating rate of 2 °C·min^{-1} from 30 °C to 210 °C and maintain this final temperature for 24 hours before the autoclave be slowly cooled to room temperature again. The light-green crystals obtained should be washed with distilled water and methanol in a centrifuge and the final product should dry at ambient temperature in a fume hood.

This experimental procedure has some process variables such as the amount of organic compound (H_2(bbdc)), the amount of nickel(II) nitrate hexahydrate, mixing temperature and temperature and time of crystallization. There are also some variables associated to the process but which amendment requires changing the real process such as the solvent of the organic compound, the amount of solvents and the wash solution.

In order to understand better the effect of this variables on the product features, there were made some trials changing some of these variables such as the amount of reagents and solvents, mixing temperature, oven temperature and time of crystallization. The conditions associated to each trial are represented in Table 3-1.

Table 3-1 – MAMS production conditions for each sample. Organic and nickel compound weight ($m_{H2(bbdc)}$ and $m_{Ni(NO3)2·6H2O}$), solvents volume ($V_{Et\ Glicol}$ and V_{H2O}), mixing temperature (T_{mix}), temperature and time of crystallization (T_{cryst} and t_{cryst}).

Label	$m_{H2(bbdc)}$	$V_{Et\ Glicol}$	$m_{Ni(NO3)2·6H2O}$	V_{H2O}	T_{mix}	T_{cryst}	t_{cryst}
A1	0.15 g	3 mL	0.3 g	12 mL	T_{amb}	210 °C	24 h
A2					70 °C		
B1	0.15 g		0.3 g		T_{amb}		
B2			0.5 g				
B3	0.21 g		0.3 g				
C1	0.15 g		0.3 g		T_{amb}		
C2					70 °C		
C3	0.15 g		0.5 g		70 °C		
C4			0.2 g		70 °C		
C5	0.09 g		0.3 g		70 °C		
C6	0.21 g				70 °C		
D1	0.15 g		0.3 g		T_{amb}		18 h
D2					70 °C		
D3			0.5 g		70 °C		
D4					T_{amb}		
D5			0.2 g		70 °C		
D6					T_{amb}		
E1	0.15 g		0.3 g		T_{amb}	180 °C	24 h
E2					70 °C		
E3	0.21 g				70 °C		
E4					T_{amb}		
E5	0.09 g				70 °C		
E6					T_{amb}		
F1	0.15 g		0.3 g		T_{amb}	210 °C	
F2			0.2 g				
F3			0.3 g				
H1	0.15 g	3 mL	0.3 g		T_{amb}		
H2		6 mL					
H3		10 mL					
I1	0.15 g	3 mL	0.3 g	12 mL	T_{amb}		72 h
I2				15 mL			
I3					70 °C		
K1	0.90 g	18 mL	1.8 g	72 mL	T_{amb}		72 h
K2				90 mL	70 °C		
O1	0.15 g	3 mL	0.3 g	12 mL	T_{amb}		24 h
O2				15 mL	70 °C		
O3	0.9 g	18 mL	1.8 g	72 mL	T_{amb}		

3.1.2. Sodium-based sorbents

Following the recommendation of the IEA GHG report [7], three samples of the sodium carbonate supported in alumina (SBSSA) were prepared. Samples were produced containing 10 wt%, 20 wt% and 40 wt% of sodium carbonate, reaching a total product weight of 5 g with distilled water as a solvent. These samples were named N10, N20 and N40 respectively.

These sorbent materials were obtained weighing the desired amount of sodium carbonate (Na_2CO_3) and dissolving it with the minimum amount of distilled water in a beaker. Then, the desired amount of alumina (Al_2O_3) was weighted in a petri dish. The carbonate solution was carefully added to the alumina with the pasteur pipette, stirring constantly with a glass rod and heating at 80 °C. This solution was then placed into the oven to dry overnight at around 90 °C. The samples were filtered in the sieves with the aid of a metal spoon in order to obtain uniform particles with a diameter range of 90-210 μm.

The experimental amounts of reagents and solvents used for each sample production are presented in Table 3-2.

Table 3-2 – Reagents and solvent weights as well as final product mass for the three carbonate samples.

Product Name	Na_2CO_3	m_{Na2CO3} (g)	m_{Al2O3} (g)	V_{H2O} (mL)	$m_{product}$ (g)
N10	10 wt.%	0.50	4.50	3	4.93
N20	20 wt.%	1.00	4.00	6	4.90
N30	40 wt.%	2.00	3.00	12	4.94

3.2. Methods

The synthetized solid sorbent materials were submitted to some characterization tests in order to define the particles structure, distribution and materials performances using the X-ray diffraction (XRD), thermogravimetric analysis (TGA), scanning electron microscopy (SEM), surface area measurement, isotherms and breakthrough measurements.

3.2.1. X-Ray Diffraction

X-Ray Diffraction – XRD, is a versatile, non-destructive analytical method with the aim of analysing the material features such as phase composition, structure, texture, among others for the powder, solid or liquid samples.

The identification of phases is reached by comparing the experimental results with some reference patterns through some available databases like the International Centre of Diffraction Data (ICDD), known as the wider database, as well as by creating new standards with pure samples [8].

The crystal structure consists of a unit cell periodically repeated and regularly arranged in three dimensions leading to a large-range order as well as clear diffraction peaks. On the other hand, the amorphous structure has only a short-range order of atoms leading to a broad humps in the diffraction pattern. Thus, crystallinity means the percentage of the crystal part in a mixture of crystalline and amorphous sample.

Powder diffractometry is a XRD technique for structural characterization of materials. This technique consists of launching X-ray beams in the sample at a certain angle (2θ), radiating it, and then these x-rays are diffracted by the phase of the sample and received by the detector giving a certain intensity.

The XRD measurements were performed on a PANalytical Empyrean diffractometer as represented in Figure 3-1. The system is equipped with a PIXcel3D solid state detector. The measurements were carried out in Bragg-Brentano geometry with a step size of 0.013° and an accumulation time of 0.54 s/step, using CuKα radiation (l=1.54187 Å).

Figure 3-1 - PANalytical Empyrean diffractometer equipped with a PIXcel3D solid state detector

3.2.2. TGA

Thermogravimetric analysis – TGA, is thermal analysis method that measures weight changes in the material as a function of temperature (or time) while the temperature is being increased at a known rate, under a controlled atmosphere.

The TGA equipment used – SETARAM TGA92-16.18 (Figure 3-2), consists of a small platinum basket connected to a very precise balance. After the sample is inside of the basket and pre-weighed, the basket is placed into a furnace with known environment (pressure, stream composition and its flow). The TGA equipment is connected to a computer, where a test is programmed on

Figure 3-2 – SETARAM TGA92-16.18 equipment

Setsoft 2000 software, describing the desired temperature range as well as the heating and cooling rates.

3.2.3. Scanning Electron Microscope

Scanning electron microscopy (SEM) is a characterization method that with a scanning electron microscope it is produced an image of the sample's surface by using a focused beam of electrons that consequently produce some signals at its surface. There are 3 basic types of signal: backscatter electrons (BSE), secondary electrons (SE) and X-rays. Then, the detection system converts them into a digital signal that is sent to the associated software on the computer.

The BSE signals are detected by a circular backscatter detector (CBS) providing element contrast images according to the atomic weight average of each compound, considering that a higher number corresponds to a "brighter" intensity of BSE [9].

The SE signals are detected by a Everhart-Thornley detector (ETD) characterizing the surface topography, i.e., this method provides information about the surface, shape and features of the sample.

The X-rays signals are detected by an energy-disperse detector that coverts the individual x-rays into electrical voltages of proportional size. The electrical pulses correspond to the characteristic x-rays of the element, being able to find the chemical composition of the samples, creating element composition maps. This technique, named Energy Disperse X-ray spectroscopy (EDS), is performed in an external equipment incorporated SEM equipment [10].

Before any analysis, the sample should be submitted to a thin carbon coating in vacuum in order to increase the samples conductivity for better signal detection.

The equipment used – *Nova NanoSEM 650* is connected to the computer that has the *xTmicroscope control v4.7.4 build 2452-msta* software (Figure 3-3). This system provides images produced by CBS and ETD detectors.

EDS analysis was performed with the *OXFORD Instruments X-Max (50mm^2)* equipment (Figure 3-3-a) incorporated in the *Nova NanoSEM 650* and its data was treated in the *INCA-Mapping* software.

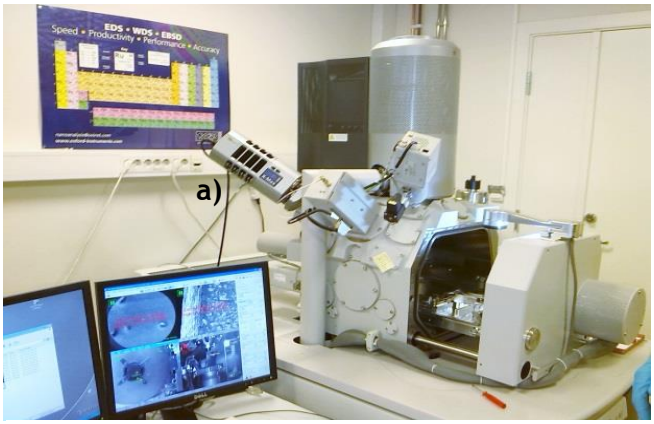

Figure 3-3 - Nova NanoSEM 650 equipment with *OXFORD Instruments X-Max (50mm^2)* incorporated (a).

3.2.4. Surface area measurement

Brunauer, Emmett and Teller – BET is a characterization method that enables the determination of specific surface area of a sample through its physical adsorption.

Stephen Brunauer, Paul Emmett and Edward Teller developed this isotherm model respecting the following assumptions [11],[12]:

1. Each adsorbed molecule provides a site for the adsorption of the molecule in the layer above it;
2. All sites on the surface have the same adsorption energy for the adsorbate, which is usually argon (Ar), krypton (Kr) or nitrogen gas (N_2) and the surface site is defined as the area on the sample where one molecule can adsorb onto;
3. Each active site can be occupied only by one particle;
4. Adsorption at each site is independently of adsorption at neighbouring sites;
5. No interactions between the adsorbate molecules;
6. Adsorbates form a monolayer;
7. Gas molecules will physically adsorb on a solid in layers infinitely;
8. The different adsorption layers do not interact;

Adsorption consists on the attachment of atoms or molecules of gas to a surface and the amount adsorbed depends on the exposed surface area, temperature, gas pressure and strength of interaction between the gas and the solid. In BET surface area analysis N_2 is usually used considering its availability in high purity and its strong interaction with most solids. The lower relative pressure is obtained by creating conditions of partial vacuum [12].

The data is treated according to the BET adsorption isotherm equation:

$$\frac{1}{\left[V_a\left(\frac{P_0}{P}-1\right)\right]} = \frac{C-1}{V_m C} \times \frac{P}{P_0} + \frac{1}{V_m C} \tag{3-1}$$

In which V_a corresponds to the volume of gas adsorbed at standard temperature and pressure (STP – 273.15 K and 1.013x10^5 Pa), in millilitres; P is the partial vapour pressure of adsorbate gas in equilibrium with the surface at 77 K (considering that it was used nitrogen as a gas stream and 77 K is liquid nitrogen boiling point), while P_0 is the saturated pressure of adsorbate gas, both in Pascal; C is de dimensionless constant that is related to the enthalpy of adsorption of the adsorbate gas on the powder sample and V_m is the volume of gas adsorbed at STP to produce an apparent monolayer on the sample surface, in millilitres.

The representation of $\frac{1}{\left[V_a\left(\frac{P_0}{P}-1\right)\right]}$ as a function of $\frac{P}{P_0}$, considering the linear part of the adsorption isotherm, results in a linear function in which $\frac{C-1}{V_m C}$ is the slope and $\frac{1}{V_m C}$ the

intercept value. Thereby, it is possible to obtain experimentally C and V_m values considering that the correlation coefficient r^2 should not be less than 0.9975.

The BET surface area - S_{BET} in m^2/g, is then determined by the following equation:

$$S_{BET} = \frac{V_m N_A A_m}{M_v} \tag{3-2}$$

In which N_A represents the Avogadro's number (6.022×10^{23} mol^{-1}); A_m is the adsorption cross section area for an adsorbed N_2 molecule (0.162 nm^2) and M_v is the molar ideal volume for N_2 (22.414 L/mol)

The isotherm measurements were performed on BELSORP-mini II equipment, with the sample pre-activated on BELPREP-vacII equipment that contains the Micro-controller X – PXR3 as a temperature controller.

3.2.5. Isotherms

The Isotherm measurements were performed on the BELSORP-max equipment (Figure 3-4), which is high performance surface area and porosity analysis instrument which has a volumetric adsorption method as a measurement principle. This equipment is connected to a computer where the results were obtained by the program BelMaster™.

The isotherm represents the evolution of the amount of adsorbate molecules adsorbed (n_a in mol/kg) with the relative pressure (p/p_0) at a constant temperature.

Figure 3-4- BELSORP-max *equipment*.

3.2.6. Breakthrough

The performance of the sodium-based sorbent supported in alumina samples: N10, N20 and N40, was analysed in a column with controlled temperature by an external oven, which exit was connected to VG ProLab with a mass range of 1-300 amu as shown in Figure 3-5. This equipment is a mass spectrometer analyser – MS. The system, shown in Figure 3-5 was programmed in the BIGCCS software as schematically represented in Figure 3-6.

The BIGCCS program is a method to control gases flow rate, valve, oven set-point temperature as well as the gases humidity (bypass or saturated, considering that it is possible to make a gas flow pass through a water recipient at constant temperature and it captures the vapour of water in equilibrium making it humid).

This system consists of 2 columns – reactor (R) and dummy (D), inside of an oven with programmable temperature; 6 different streams that, after passing through their mass flow controllers, connected to just one stream – *line 1*, and one stream of N_2 that after its mass flow controller is named *line 2*; one valve; one saturator responsible for providing the water to the system (humidity); 4 thermocouples (inside of the reactor) and a MS analyser.

Figure 3-5 - Breakthrough measurements system.

The reactor can be fed by a humid or dry stream choosing the valve position – through saturator or bypass, before entering the column. However, the stream that feeds the Dummy has to be dry.

The 6 possible gas feeds that join *line 1* are: N_2 , *Mix*(CO_2), CH_4, H_2, *CO* and *Ar*. However the second one is the most used – *Mix*(CO_2) constituted by 90.09 % of N_2 and 9.91 % of carbon dioxide (CO_2).

The filling of the reactor (R) - Figure 3-7, starts to place the tube *b)* into column *a)* in order to support the sample that stays around the middle of the column. Then, the filter *c)* is placed properly thus, it does not turn and after, it should be put some quartz wool on the filters top to protect the system, followed by the pre-weighed sample. Then, the tube that supports the thermo elements (*e*) can be placed, carefully inside of the tube, taking care not to damage the sample, followed by the thermo elements (*f*) and to finish the connection at the end of the column to connect the tube to *MS* analyser as well as exhaust.

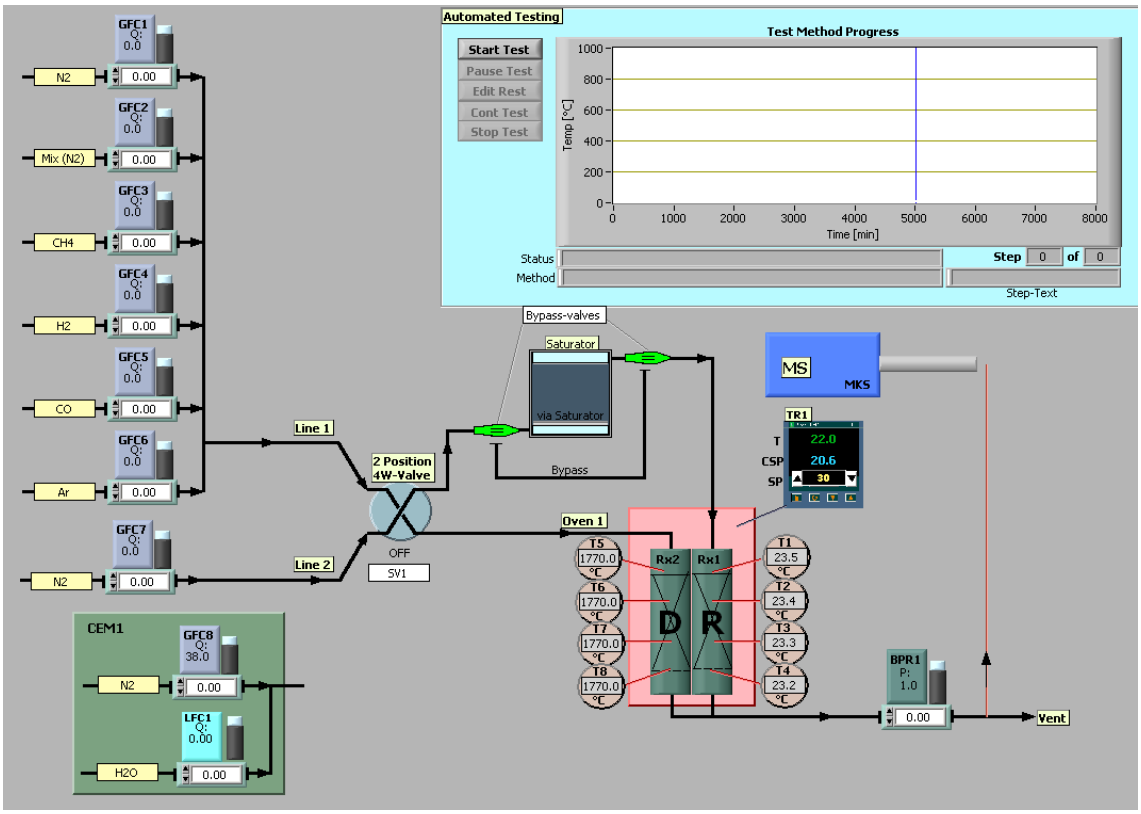

Figure 3-6 – BIGCCS programme with a scheme of breakthrough curve measurement.

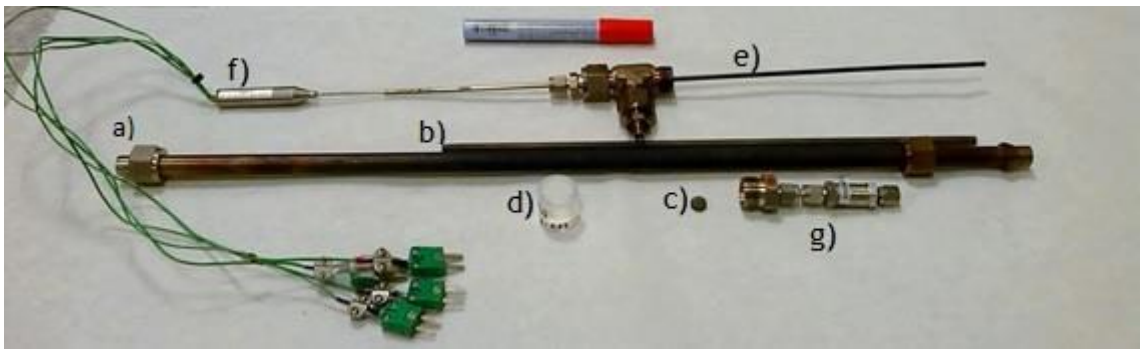

Figure 3-7 – a) Column used on the sodium-based sorbent samples tests; b) tube to support the sample inside of the column; c) filter to put on the top of "b" element; d) sample N10 placed inside of a glass container; e) tube to support the thermocouples inside of the column; f) metal tube with four thermocouples; g) connection between the end of the column and the MS tube.

The MS analyses the exit of the column and reads the signal in intensity, saving the data considering 18, 28, 32 and 44 as ionization numbers for H_2O, N_2, O_2 and CO_2 respectively.

In order to analyse the data in terms of percentage of each gas, the read signal, in intensity, was divided by the sum of all signals at each time.

$$y_i = \frac{Intensity_i}{\sum Intensity_i}$$

(3-3)

The total molar concentration at the entrance of the column is determined using the ideal gases law (equations 3-4 and 3-5).

$$PV=nRT$$

(3-4)

$$C_E=\frac{P_E}{RT_E}$$

(3-5)

In which C_E, P_E and T_E represents the total molar concentration, pressure and temperature at the entrance of the column, respectively and R is the constant of ideal gases.

The molar concentration of each gas at the entrance of the column, can be obtained multiplying C_E by the feed percentage of this gas, as shown in the follow equation:

$$C_{0,\,i}=C_E \times y_{0,i}$$

(3-6)

Likewise, the molar concentration of each gas, at each recorded time, can be obtained by multiplying C_E by the gas percentage at the same time, as shown in the follow equation:

$$C_i=C_E \times y_i$$

(3-7)

If the breakthrough curve was an ideal stoichiometric front, the same amount of solute that enters the column would be retained during the stoichiometric time, t_{est}:

$$Q\ C_0\ t_{est}=Q\int_0^\infty \left(1-\frac{C}{C_0}\right)dt \ <=> t_{est}=\int_0^\infty \left(1-\frac{C}{C_0}\right)dt$$

(3-8)

The total capacity of the material, i.e., the total amount of solute adsorbed until complete exhaustion, q_{total} is then obtained by the following equation.

$$q_{total}=\frac{C_0\,Q\int_0^\infty \left(1-\frac{C}{C_0}\right)dt}{m_{ads}}$$

(3-9)

4 Results and discussions

4.1. MAMS

The yield based on the ligand $(H_2(bbdc))$ is shown in Figure 4-1 as a function of the reagents amounts and mixture temperature. On these samples (A1 to C6, F1 to F3 and H1) it was maintained the total amount of solvent (15 mL) and the crystallization parameters (24h, 210 °C).

The ligand is the limiting reagent, thus it was expected the yield increases with the amount of ligand at ambient temperature as mixing parameter. However, increasing the mixing temperature to 70 °C, the yield decreased with the ligand amount beyond the reference quantity. On the other hand, these two samples (prepared with more amounts of organic and at both of mixing temperatures – B3 and C6) have the same XRD results matched not only with the reference trial but also with the supporting information [13]. The TGA analysis was not possible for the sample C6 because of the total quantity of product; however the B3 sample fitted with the reported results, differing only in 5 % over the final percentage of compound left.

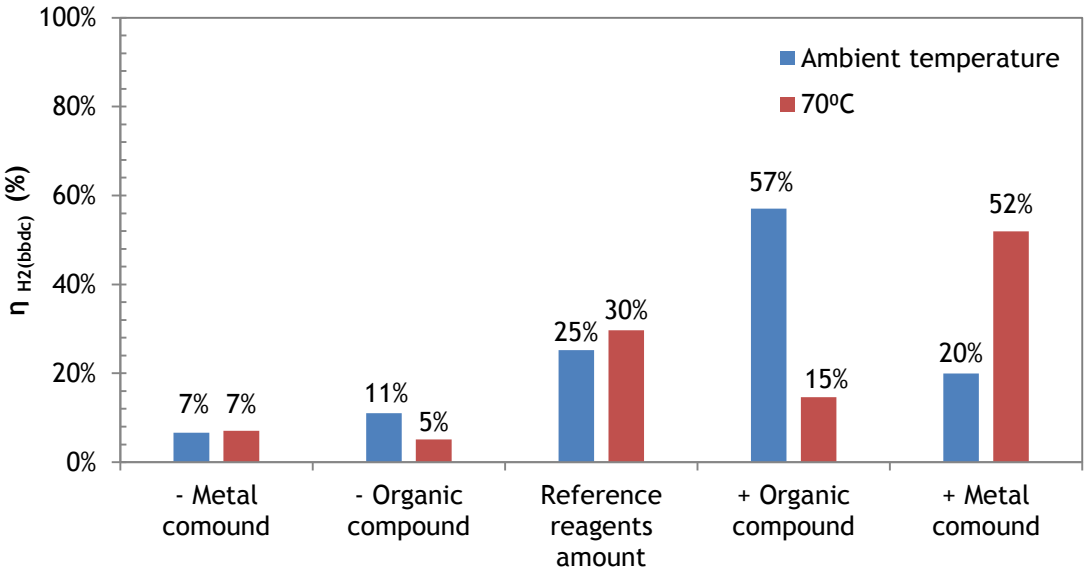

Figure 4-1 –Yield of samples A1 to C6 and F1 to H1 according to reagents amount and mixing temperature, maintaining the amount of solvent (15 mL) and the crystallization parameters (24 h, 210 °C).

The change in the amount of metal compound $(Ni(NO_3)_2 \cdot 6H_2O)$, at 70 °C as mixing temperature – samples C4, C2 and C3, causes an increase in yield. However the XRD and TGA

analysis of the sample C3 (better yield), has not matched properly with the reference results [13] even though presenting the expected appearance. Using ambient temperature as a mixing parameter, it was noticed that the decrease of the nickel compound (F2) compared to the reference (F1), is directly proportional to the yield. On the other hand, the increase of this metal compound (B2) compared to the F1 not only causes a decrease of the yield as it has also a not matched TGA result with MAMS-1 [13].

The produced samples A1, B1, C1, F1 and H1 using ambient temperature as a mixing parameter and using the reference reagents ratio, were selected as having the best match between the XRD and TGA analysis as well as good reproducibly.

The change on the amount of solvent, was made at ambient temperature as a mixing parameter, and it was crystallized during 24 hours at 210 °C. On these samples (H1, H2 and H3) it was maintained the reagents and distilled water reference amounts. The yield result as a function of ethylene glycol volume is presented in Figure 4-2.

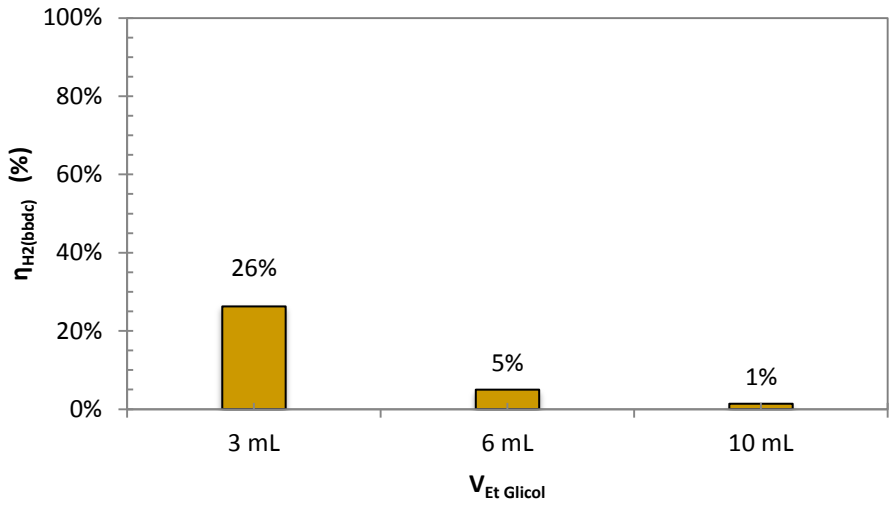

Figure 4-2 – Yield of samples H1, H2 and H3, according to the volume of solvent, maintaining the reference reagents ratio, mixing temperature (T_{amb}), crystallization parameters (24h, 210 °C)

The product obtained with 6 mL of ethylene glycol (H2) was a grey gel and the one with 10 mL (H3) was grey powder with some black particles. The total product obtained in both of them was too small for XRD and TGA analysis.

The change in the crystallization temperature to 180 °C, maintaining the other variables constant, had no effect since no product was found – samples E1 to E6. Thus, it was evaluated the crystallization time for trials with the reference reagents ratio maintaining the

crystallization temperature at 210 °C, changing with the mixing temperature as shown in Figure 4-3.

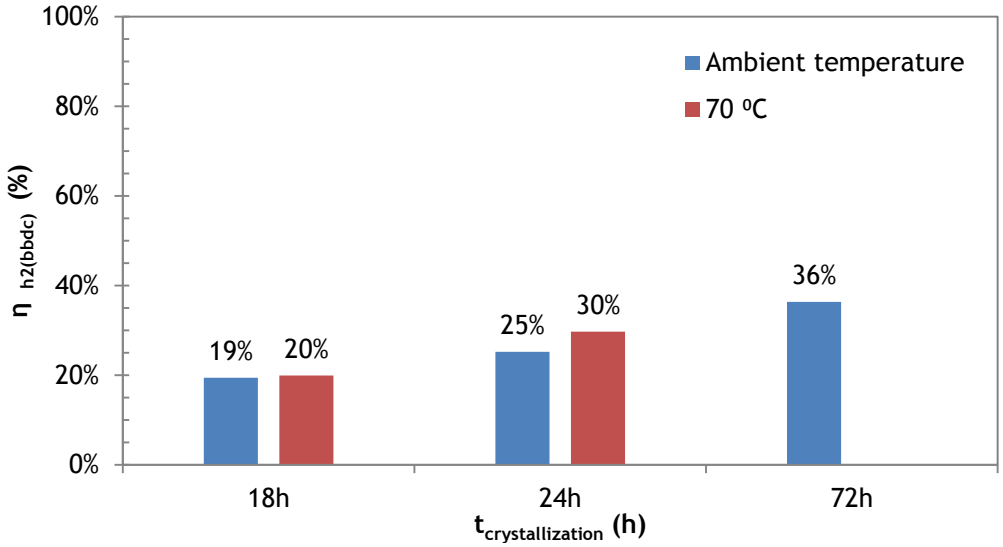

Figure 4-3 - Yield of samples A1, A2, B1, C1, C2, D1, D2, F1, H1 and I1 according to crystallization time - $t_{crystallization}$, and to the mixing temperature, maintaining the reference reagents ratio, volume of solvent (15 mL) and the crystallization temperature (210 °C)

The yield increase with the cooking temperature for these samples at both mixing temperatures, however, at 70 °C it is slightly higher than the one at ambient temperature. Considering that the mixing temperature does not make a noticeable difference, it was decided to produce sample I1 in larger amounts (produced with ambient temperature as a mixing parameter).

After changing some process variables on these tests (reagents ratio, mixing temperature, volume of ethylene glycol solvent as well as time and temperature of crystallization) and before testing sample I1 in larger amounts, two trials were performed producing it with only water as a solvent – I2 and I3 which results are shown in Figure 4-4.

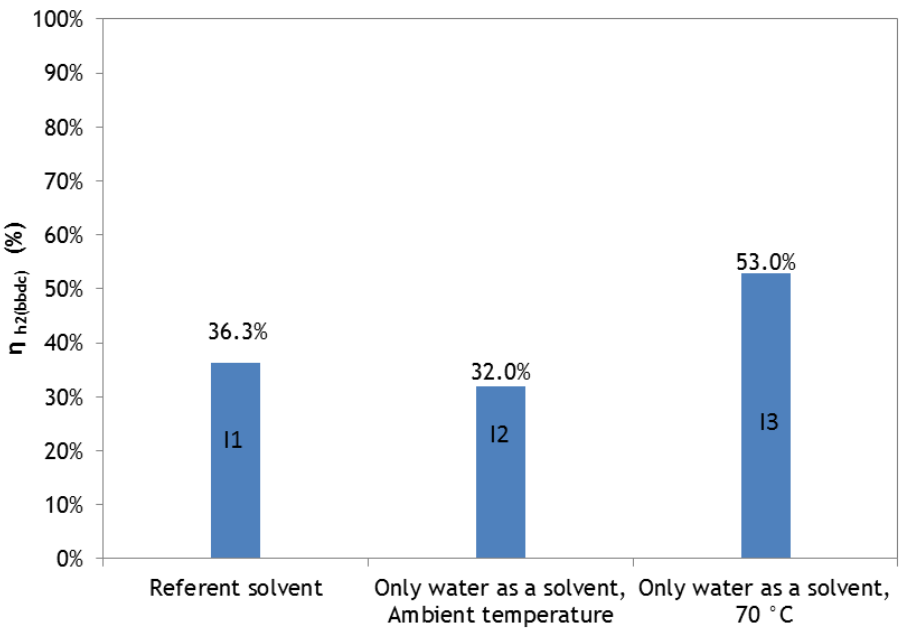

Figure 4-4 - Yield of samples I1, I2 and I3 according to the mixing temperature and type of solvent, maintaining the reference reagents ratio, total volume of solvent (15 mL) and the crystallization parameters (72 h, 210 °C).

The sample I3, made just with water as a solvent and at 70 °C as a mixing temperature, is the highest, however the product formed was a brown needle-like crystal with a very few light-green needle-like crystals, while the sample I1 is a light-green needle-like crystal as reported [1]. On the other hand, the sample I2, made also just with water as a solvent but at ambient temperature as a mixing parameter, looked completely brown. These brown crystals are assumed to be mainly result of the ligand precipitation as suggested by Shengqian Ma et al. [1]. However, the XRD results for I3 sample matched with the reported one with just a slightly different on the second peak intensity.

Then, it was decided to produce samples I1 and I3 in larger amounts - samples K1 and K2 - in order to produce around 0.20 g/batch instead of just 0.05 g/batch. These larger samples were produced with the same ratio between the reagents and solvent as the smaller ones and crystallized at 210 °C for 72 h. The yield results for smaller samples (I1 and I3) and larger samples (K1 and K2) are shown in Figure 4-5.

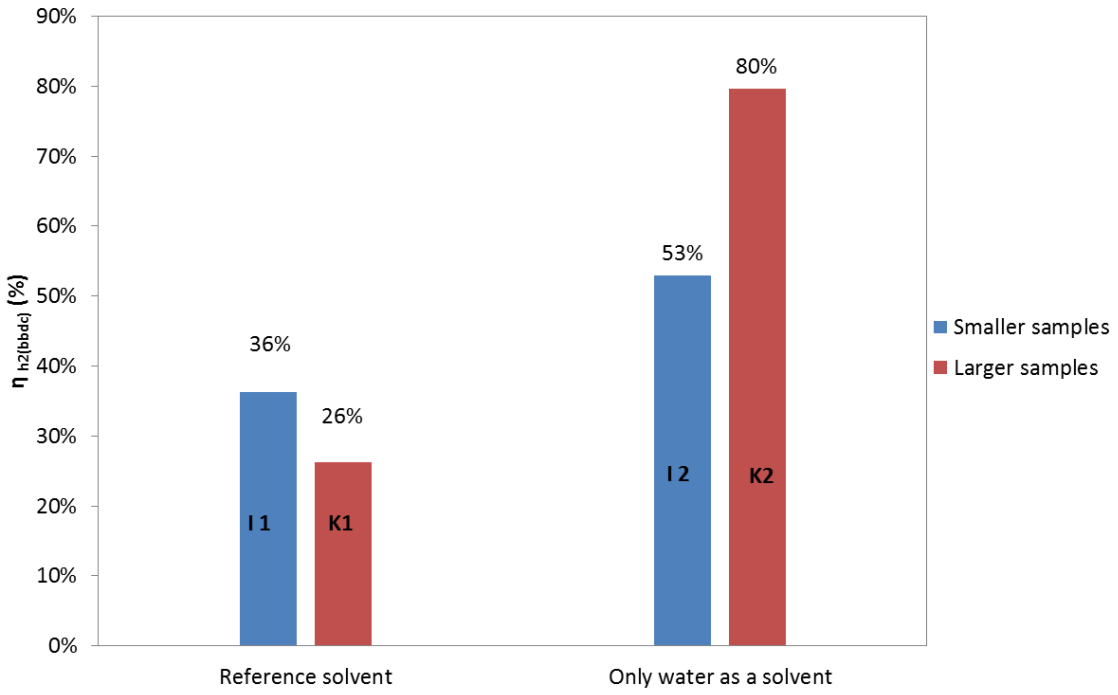

Figure 4-5 - Yield of smaller samples (I1 and I3) and larger samples (K1 and K2) according with the type of solvent used, maintaining reference reagents ratio as well as solvents ratio, and the crystallization parameters (72 h, 210 °C).

The samples I1 and K1 have the same appearance. The XRD result for both samples obtained by Highscore plus software, were compared to the expected reported result [13] as shown in Figure 4-6 and Figure 4-7.

In these figures, the blue line corresponds to samples I1 and K1, respectively, while the red and green lines correspond to fresh sample and activated at 200 °C [13], respectively. As shown in Figure 4-6, there is a match between the reported fresh sample and the sample I1, not only on the peaks position but also on their intensity, making it possible to assert that these particles are the same. In Figure 4-7 it is possible to see the same resemblance although there is just a small difference in the intensity of the second peak that could be associated to their packing for the characterization test.

The small and larger XRD results were compared with each other as shown in Figure 4-8.

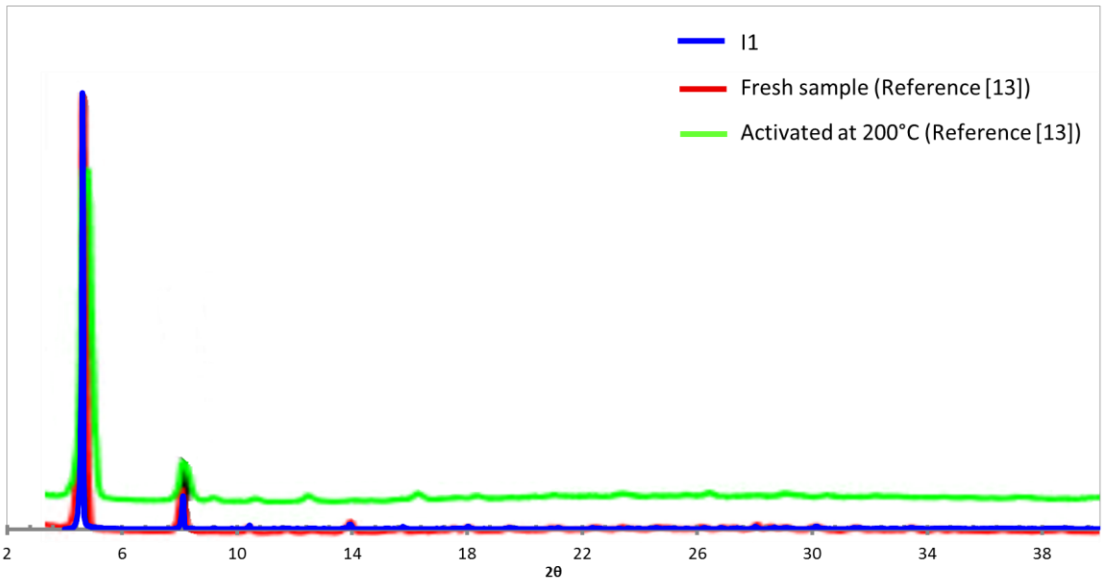

Figure 4-6 - XRD results for sample I1 (blue), MAMS-1 fresh sample [13] (red) and activated at 200 °C [13] (green).

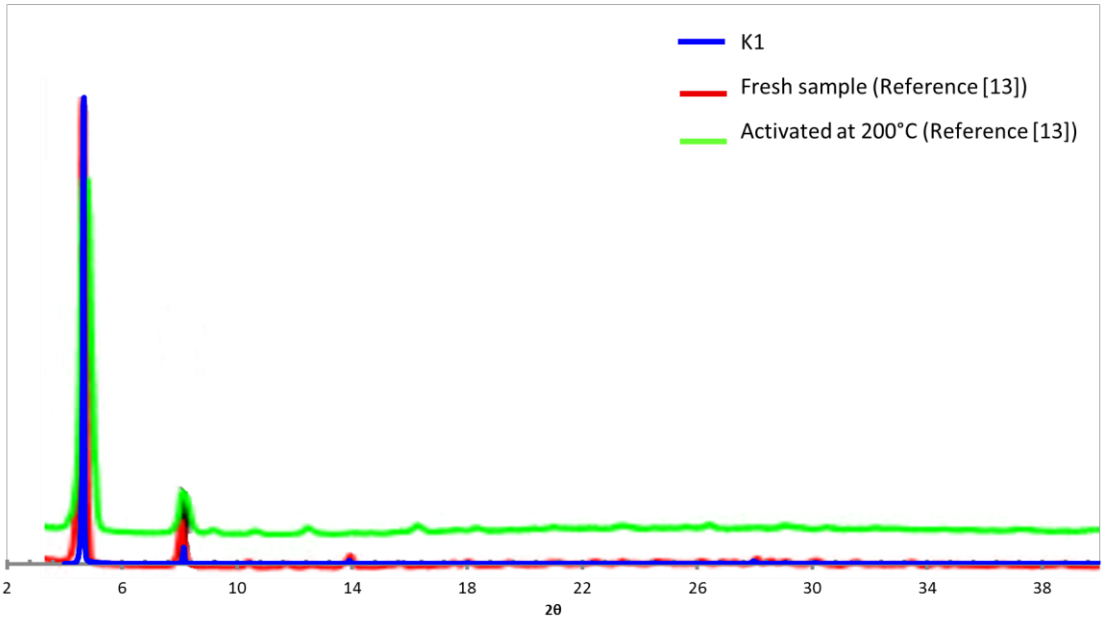

Figure 4-7 - XRD results for sample K1 (blue), MAMS-1 fresh sample [13] (red) and activated at 200 °C [13] (green).

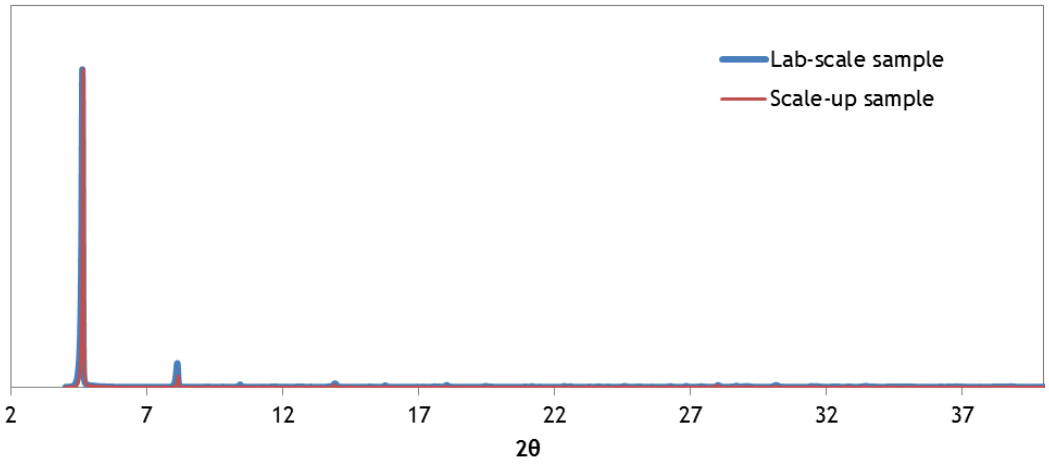

Figure 4-8 – XRD results for the sample I1 (blue line) and K1(red line).

As can be seen, both results show peaks on the same positions. Considering that the peaks position is a periodic arrangement indicative, it is possible to say that samples I1 and K1 have the same arrangement. The slightly difference between both XRD results on the second peak intensity, does not have relevant meaning, because it could be just related to the amount analysed or even the samples packing for the characterization test.

On the other hand, samples I3 and K2 had a completely different appearance. The I3 sample, as previously described, appear like brown needle-like crystal with a very few light-green needle-like crystals while K2 sample appear like very light-green big needle-like crystal as shown in Figure 4-9.

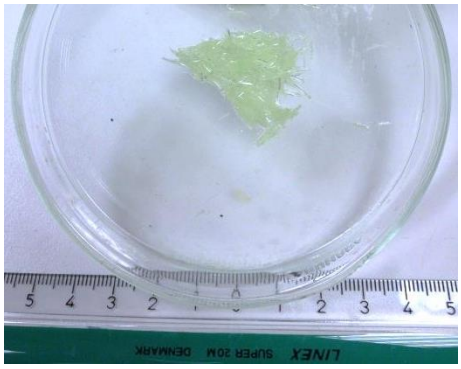

Figure 4-9 – Picture of K2 sample made just with distilled water as a solvent and referent reagents ratio, mixing temperature at 70 °C, crystalized at 210 °C for 72h.

The XRD results for K2 sample were completely different comparing with the reported one and with I1 and K1 samples. Its results show the main peaks at different positions, intensity and total amount.

TGA analysis of produced samples, was performed with the equipment shown in Figure 3-2, under 50.0 mL/min flow of N_2 in a temperature range 20-550 °C (heating rate 2 °C/min). Considering that the balance system of SETARAM TGA92-16.18 was quite sensitive, the tests in this equipment were performed with higher initial weight of sample as the reported one (25.2 mg and 41.9 mg for I1 and K1 samples, instead of 9.8 mg as reported [13]). The results for these three samples are presented in Figure 4-11.

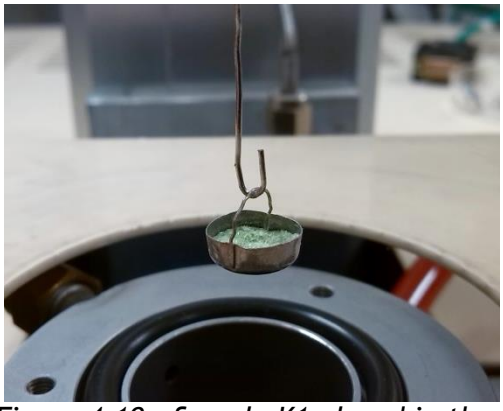

Figure 4-10 - Sample K1 placed in the platinum basket at furnace entrance of SETARAM TGA92-16.18 equipment.

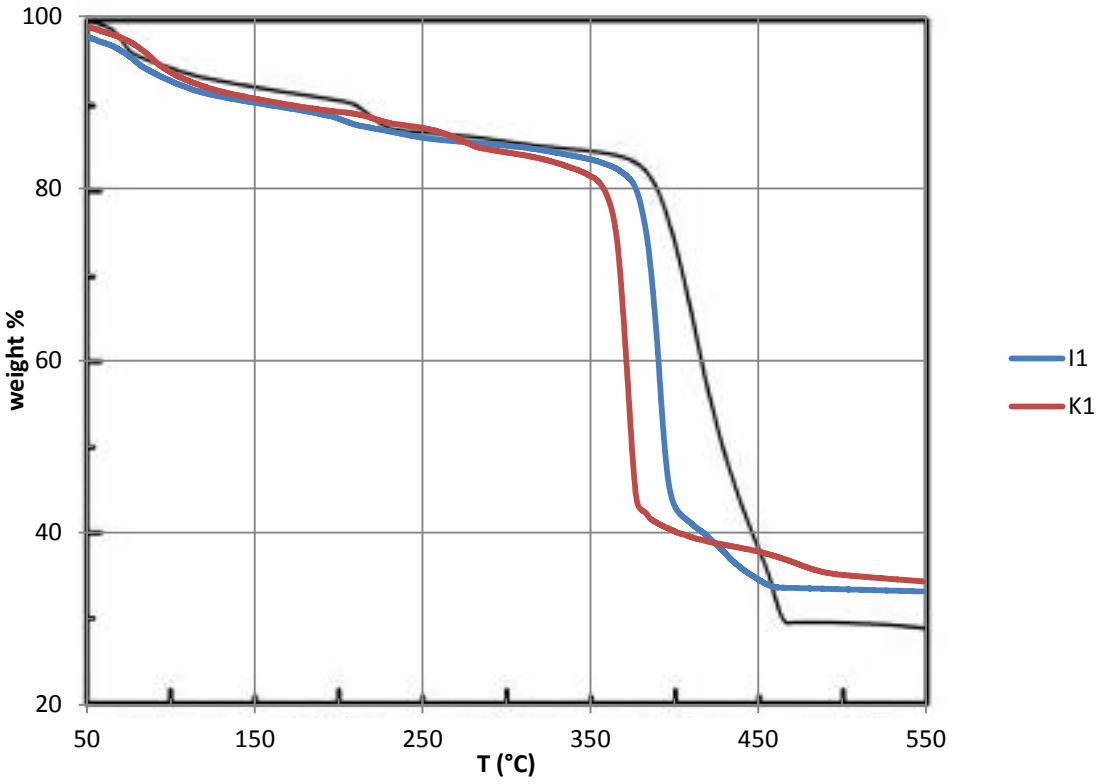

Figure 4-11 - TGA for produced MAMS samples (I1: blue, K1: red) and reference curve (black) [13].

The first weigh loss of approximately 10 % from 50 °C to 150 °C corresponds to the loss of free H_2O molecules, followed by the weight loss of approximately 6 % from 150 °C to 350 °C

corresponding to the loss of coordinated H_2O molecules. Further than 400 °C, both frameworks (I1 and K1) decompose completely. The final weight percentage should represent the nitrate oxide and some organic compound polymerized.

At the end, both experimental frameworks stayed with approximately 33-34 % of the initial weight whereas the reference result ended with approximately 29 % of the initial weight [13]. This difference between experimental and reported samples may be due to the heating rate which was not supplied. On the other hand, both experimental TGA results, for samples I1 and K1, have some differences. The biggest weight loss in short time (slope in the curve presented in Figure 4-11) of K1 and I1 samples differs in 20 °C, i.e., the I1 sample start to decompose at 20 °C after K1 and it ended at less 2 % of the initial weight.

Even with this dissimilarity on the TGA slope it is not possible to assert that I1 and K1 samples are different, considering that they also have the same appearance and quite the same XRD result.

On the other hand, the TGA result for K2 sample was completely different from I1 and K1 samples as well as the reported result. K2 sample results just show one big slope around 250 °C and it ended at around 3 % of the initial weight.

A surface area measurement was performed to I1, K1 and K2 samples by measuring the isotherm of each sample with N_2 at 77 K on BELSORP-mini II equipment. The measured samples (I1, K1 and K2) were previously activated at 200 °C, with 2 °C/min as heating rate, overnight under vacuum on the BELPREP-vacII equipment that is a gas/vapour adsorption pre-treatment instrument that contains the Micro-controller X – PXR3 as a temperature controller. The isotherm result is represented in Figure 4-12.

The isotherm points at low relative pressure, of each isotherm (before the Inflexion point), are represented in Figure 4-13 as well as its trend line according to equation 3-1.

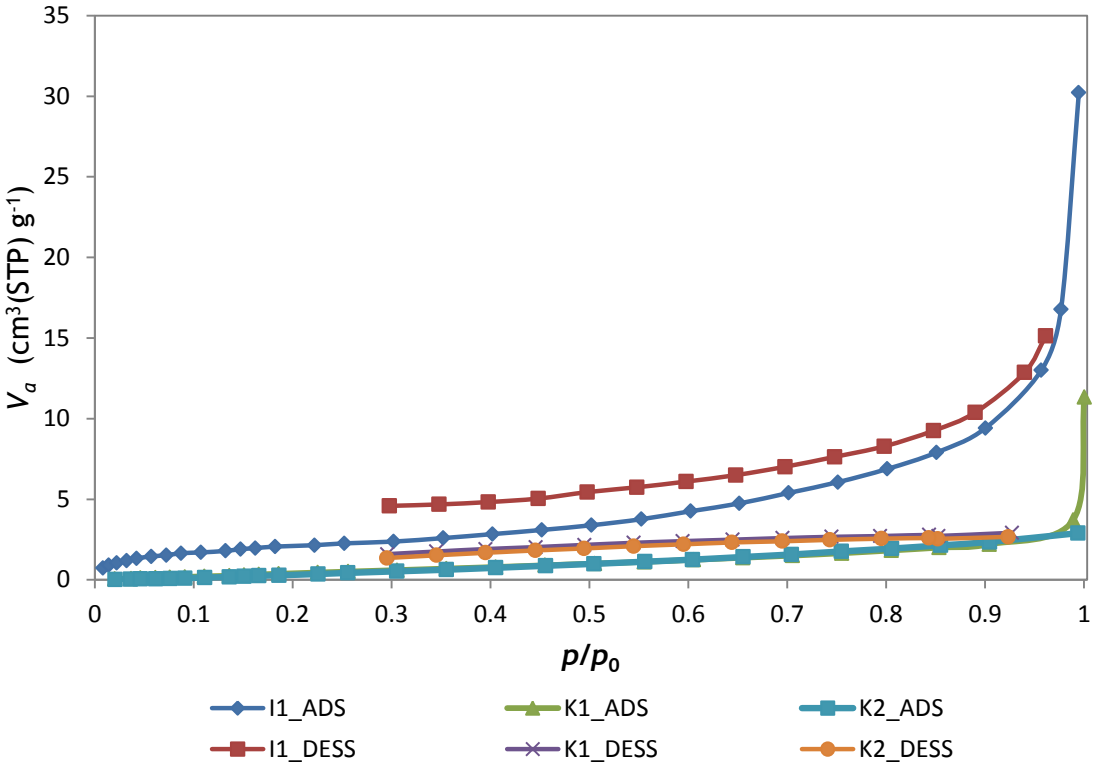

Figure 4-12 - Adsorption/desorption isotherms for MAMS samples - I1, K1 and K2, performed with N_2 at 77K on BELSORP-mini II equipment.

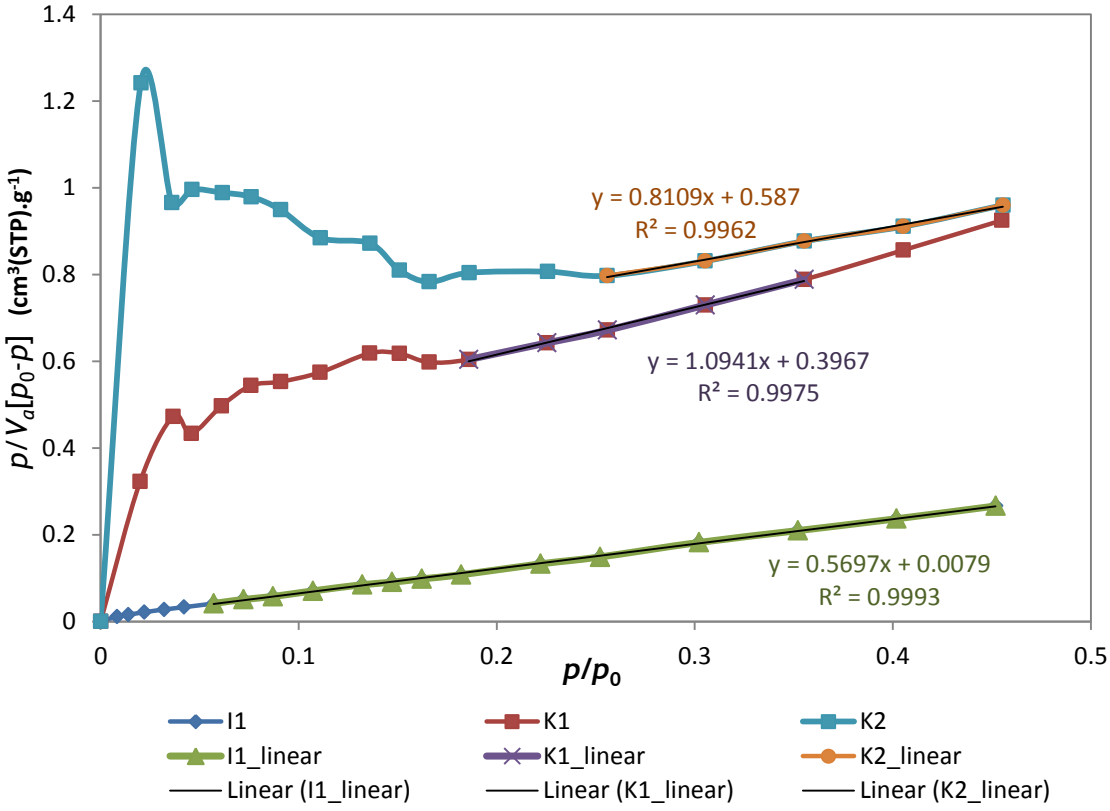

Figure 4-13 - BET plot for MAMS samples - I1, K1 and K2, performed with N_2 at 77K performed with N_2 at 77K on BELSORP-mini II equipment.

The results according to the equations 3-1 and 3-2 are presented in Table 4-1.

Table 4-1 – BET results for MAMS samples – I1, K1 and K2.

MAMS	$m_{anlysis}$ (g)	V_m (cm^3(STP)/g)	C	S_{BET} (m^2/g)
I1	0.02	1.73	72.77	7
K1	0.04	0.67	3.76	3
K2	0.04	0.72	2.38	3

According to the result for the volume of gas adsorbed at STP to produce an apparent monolayer on the sample surface (V_m) as well as the surface area of the sample (S_{BET}), it is concluded that I1 sample has larger surface area and consequently bigger $V_{m.}$. The results for K2 sample are not so trustable due to its correlation coefficient that is smaller than 0.9975 as presented in Figure 4-13.

Another K1 sample was submitted to an isotherm adsorption measurement of N_2 at 77 K on BELSORP-max equipment. The sample was previously activated at 200 °C, with 2 °C/min as heating rate, overnight under vacuum on the BELPREP-vacII equipment and reactivated on the BELSORP-max at 200 °C, with 2 °C/min as heating rate for 14 hours. The desired adsorption temperature – 77 K, was maintained with the aid of an external liquid nitrogen bath. Isotherm result showed that any N_2 gas molecule was adsorbed on the sample.

Then, it was made another measurement with the same sample but testing the carbon dioxide (CO_2) adsorption at 253 K, reactivating the sample again on the BELSORP-max at 200 °C, with 2 °C/min as heating rate for 14 hours. However, the results showed that any CO_2 molecule was also adsorbed on the sample.

Unfortunately it was not possible to measure the I1 CO_2 adsorption because the equipment was not available. However, one of the authors of MAMS' article was contacted by e-mail in order to clarify some results and doubts. Regarding the larger sample (K1), Shengqian Ma. said "I encountered some difficulties to scale-up to larger than even 0.1 g/batch (…) I used multi-autoclaves to scale it up.".

4.2. Sodium-based sorbents

The sodium-based sorbent supported in alumina samples (N10, N20 and N40) were submitted to some characterization tests in order to obtain information about their crystallinity and possible presence of secondary products – XRD; sodium carbonate distribution on the alumina

surface as well as samples' shape, appearance and element distribution – SEM analysis and EDS; and the surface area of the samples – BET. Then, samples performance was tested with a breakthrough measurement inside of a column.

The XRD results obtained by Highscore plus software, for N10, N20 and N40 samples are represented in Figure 4-14. This software with the ICDD data base enables the identification of some expected components in the material according to the equations 2-4 to 2-6 [5] as shown in Figure 4-15.

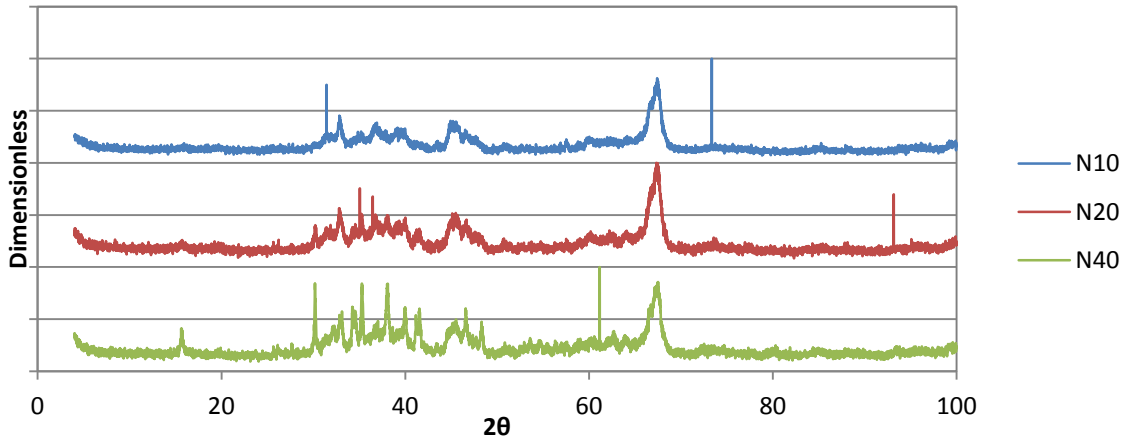

Figure 4-14 - XRD results for samples N10 (10 wt.%), N20 (20 wt.%) and N40 (40 wt.%) obtained by Highscore plus software.

For these particles, there was not a reference result to compare with. However, the results shows that, as expected, the sodium carbonate signal increase with the amount of this compound in the sample (N10 to N40) and it is also possible to see the sodium bicarbonate presence which implies that at least the secondary reaction, represented by the equation 2-4, occurs at this production conditions.

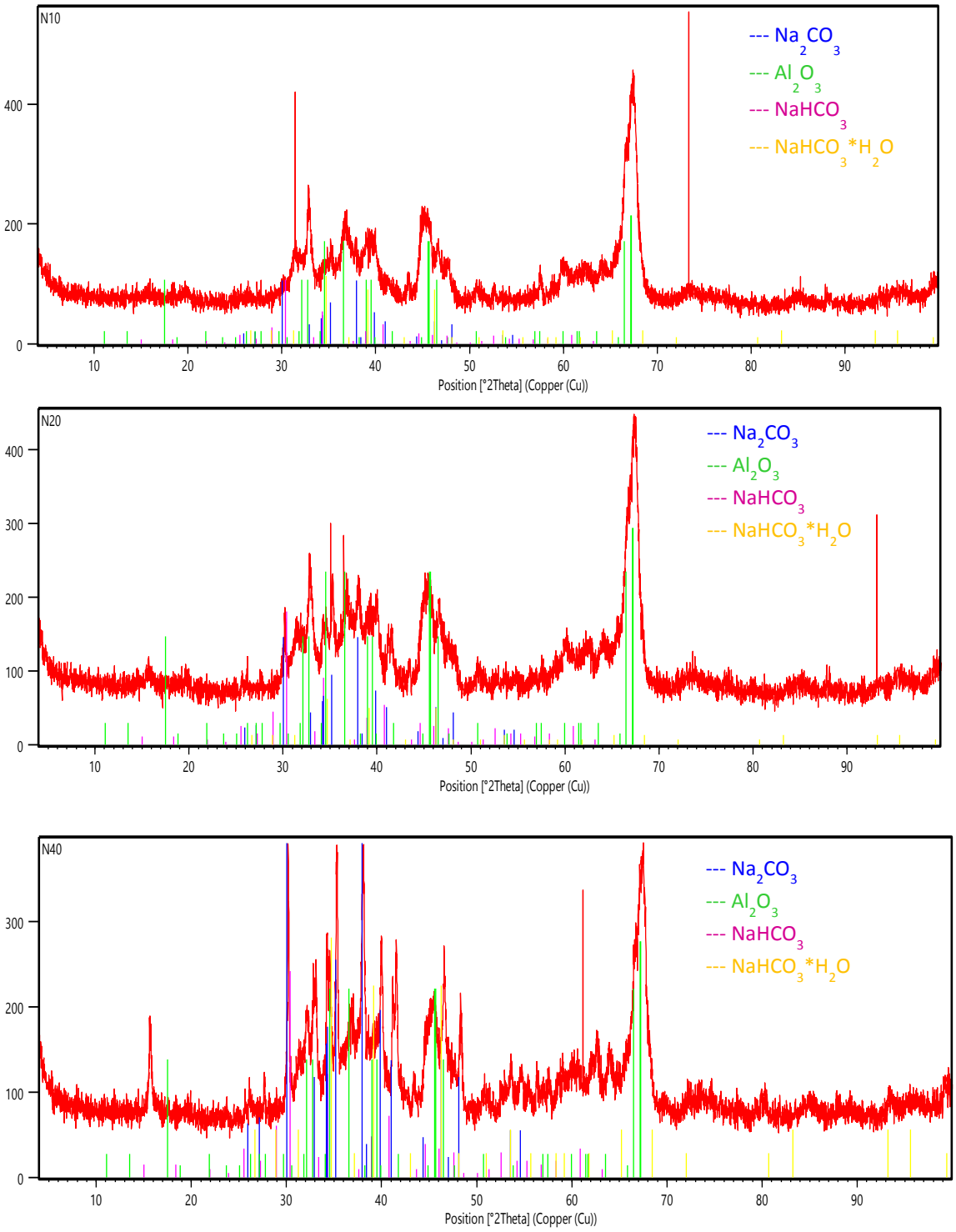

Figure 4-15 - XRD results for samples N10 (10 wt.%), N20 (20 wt.%) and N40 (40 wt.%) obtained by by Highscore plus software with the ICDD data base.

Posteriorly there was made a SEM analysis in order to understand the sodium carbonate dispersion in alumina surface. The images produced by CBS and ETD detectors are presented in Figure 4-16 and Figure 4-17, respectively.

The expected compounds in the samples were sodium carbonate (Na_2CO_3) with 106 g/mol as a molecular weight and 20 as a molecular atomic weight average; and alumina (Al_2O_3) with 102 g/mol as molecular weight and 17 as a molecular atomic weight average. Considering the proximity of molecular atomic weights, it is not obvious the perception of their positions on CBS images, however it is expected that the "brighter" part of the image is associated to the alumina due to its higher atomic number. The background of the image corresponds to the carbon tape where it was placed the sample (with 12 as atomic weight average number). Among the three analysed samples, it is not possible to distinguish them so much only with CBS images because of the proximity of elements atomic numbers.

The ETD images show the shape of the samples providing the idea of approximately spherical particles with a diameter around 100 μm for the three of them which was also the size of alumina used.

However, only SEM images are not enough to describe the material and to understand if the sodium carbonate is really disperse in the alumina surface and the difference between the samples. In order to answer to these questions, it was carried out EDS analysis with the OXFORD Instruments X-Max (50 mm^2) equipment incorporated in the Nova NanoSEM 650 (Figure 3-3) in which the data was treated in the INCA-Mapping software. With this technique, Al, Na, O and C are detected. As shown in Figure 4-18 to Figure 4-20 it is possible to see the dispersion of Na and Al in each particle in the sample according to the light colour in the images b and c.

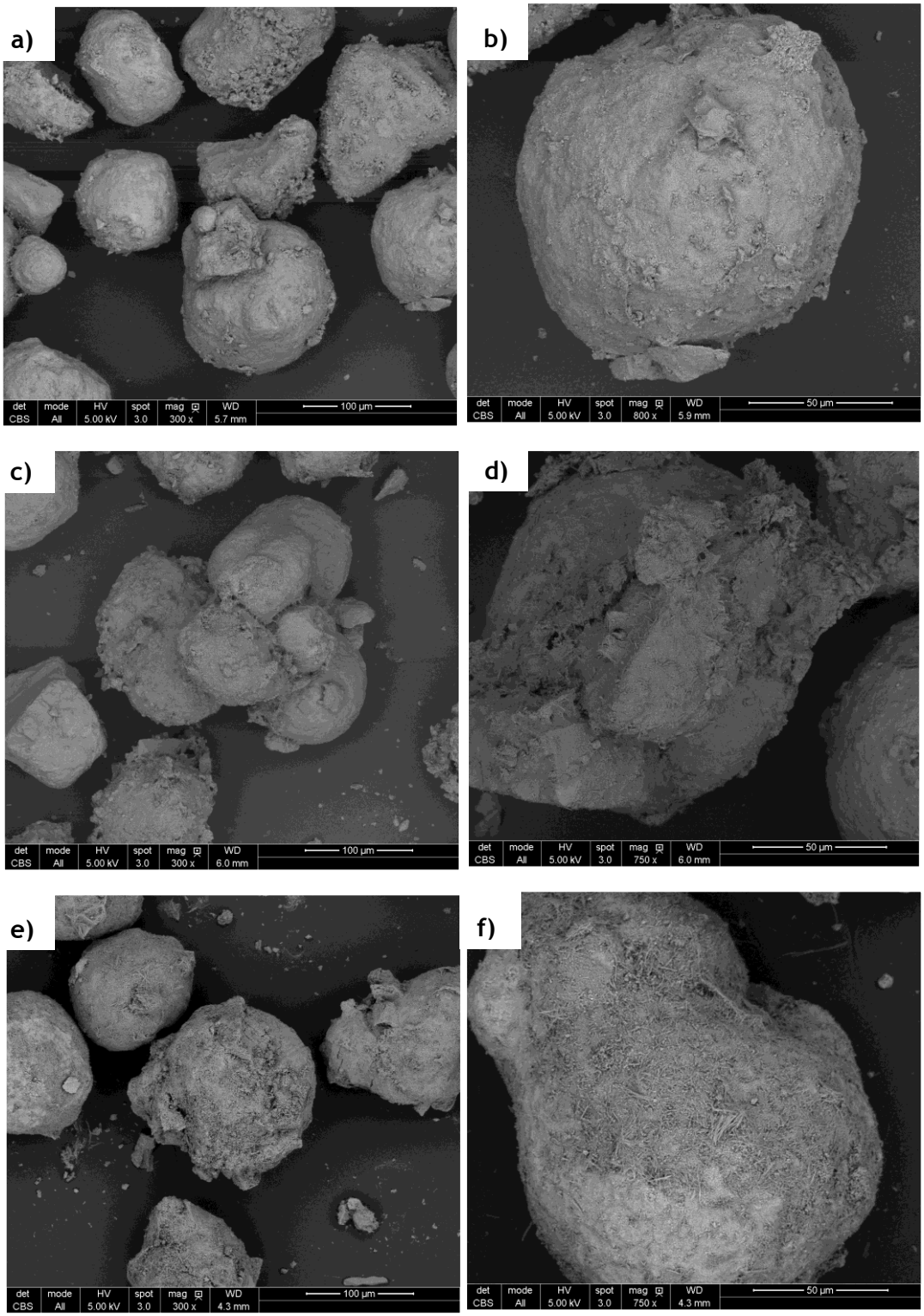

Figure 4-16 - CBS images of sodium-based sorbent supported in alumina samples. a), c) and e) represent the images for N10, N20 and N40 respectively with a magnification of 500 times. b), d) and f) represent the images for N10, N20 and N40 respectively with a magnification of 750 times.

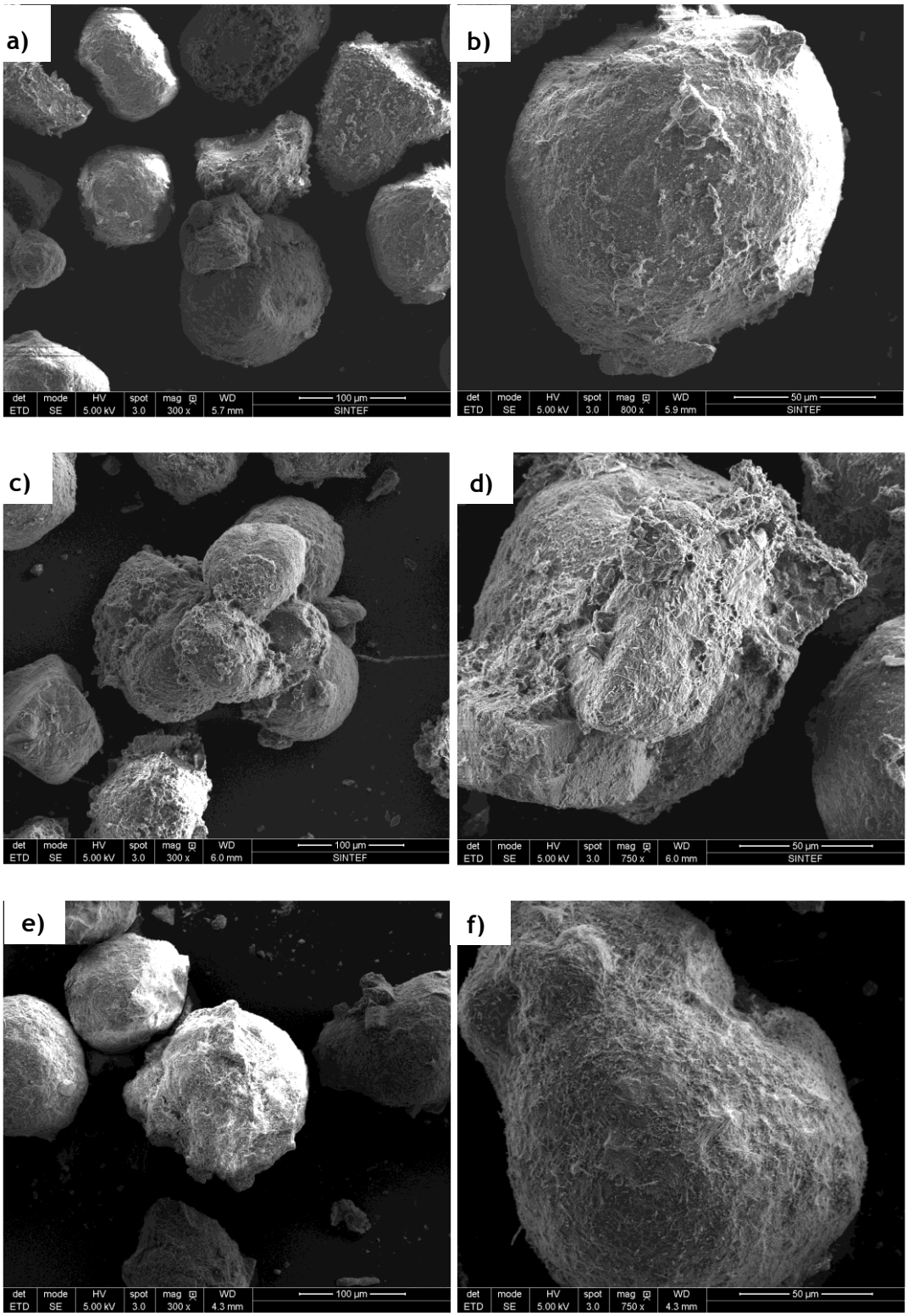

Figure 4-17 - ETD images of sodium-based sorbent supported in alumina samples. a), c) and e) represent the images for N10, N20 and N40 respectively with a magnification of 500 times. b), d) and f) represent the images for N10, N20 and N40 respectively with a magnification of 750 times.

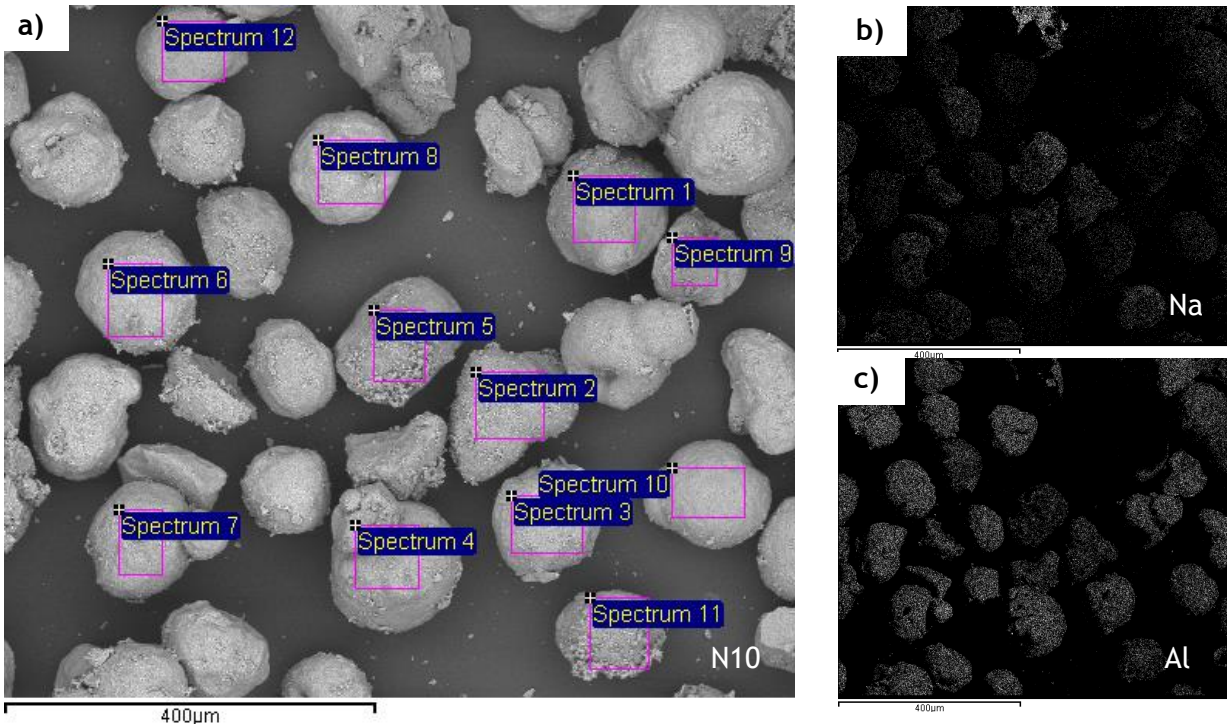

Figure 4-18 - EDS images of N10 sample. a) reference image; b) element intensity map of sodium (Na); c) element intensity map of aluminium (Al).

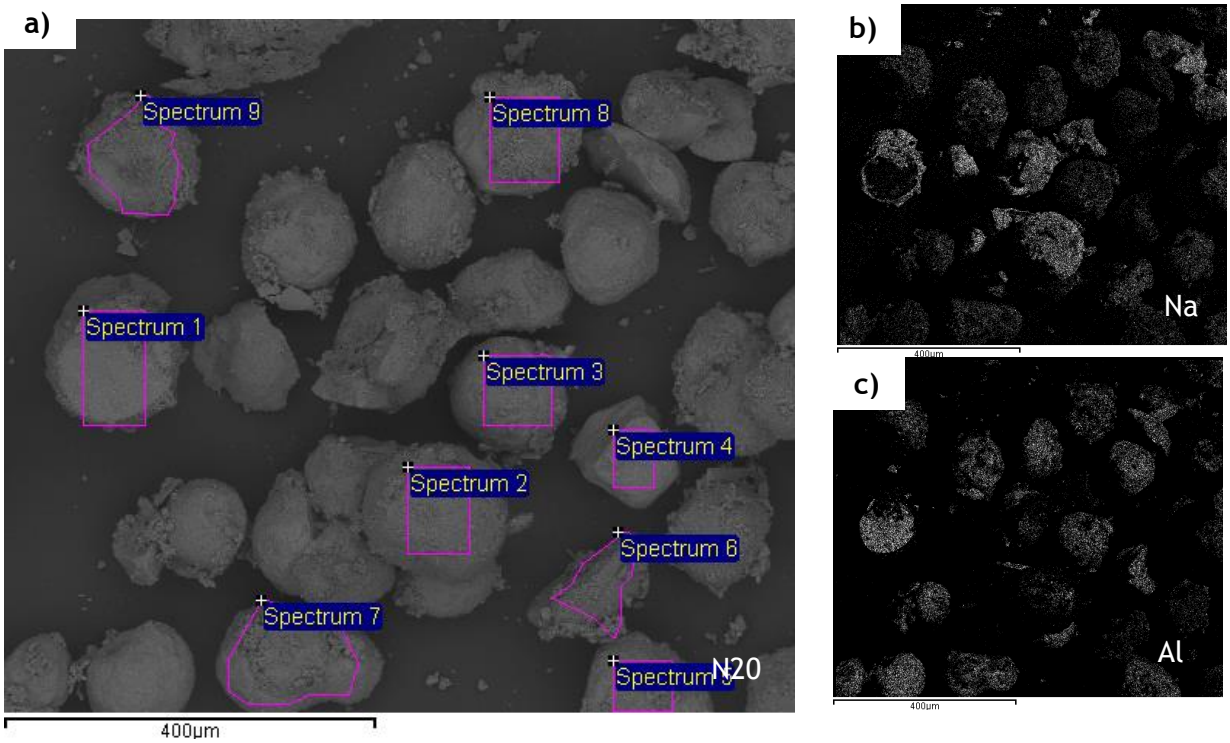

Figure 4-19 - EDS images of N20 sample. a) reference image; b) element intensity map of sodium (Na); c) element intensity map of aluminium (Al).

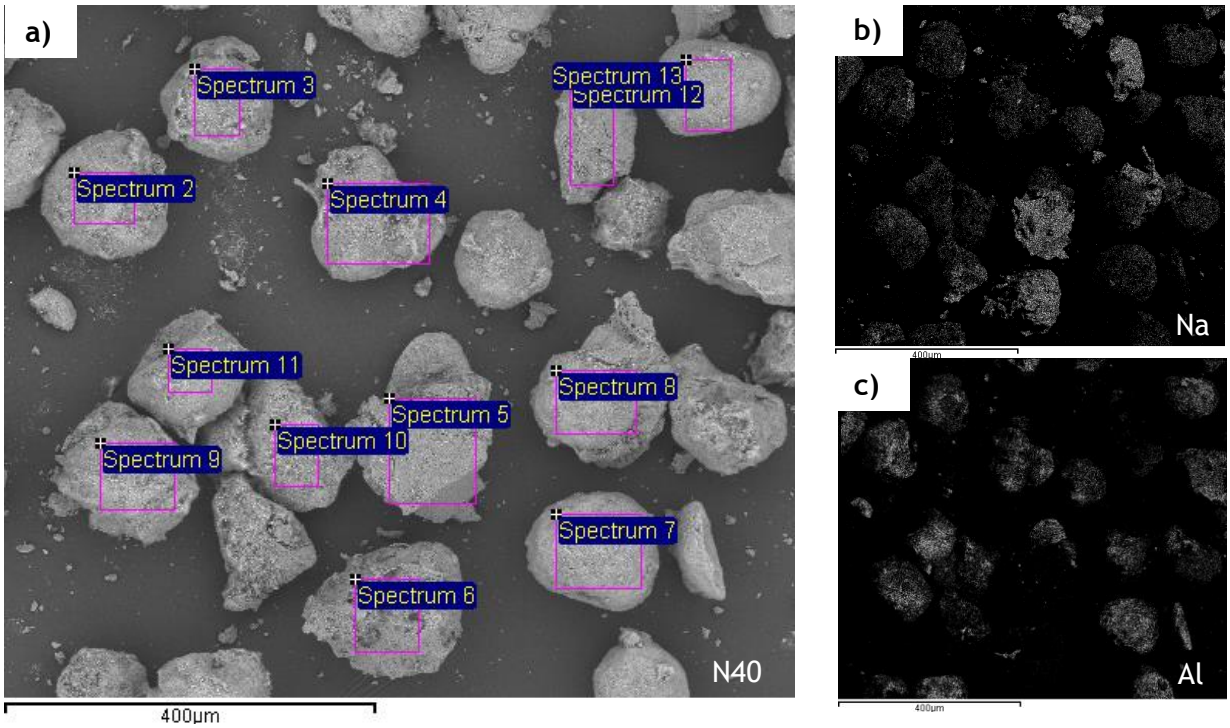

Figure 4-20 - EDS images of N40 sample. a) reference image; b) element intensity map of sodium (Na); c) element intensity map of aluminium (Al).

With these images (b and c) it is possible to verify an increase in the amount of sodium, from the N10 sample to N40 as well as a decrease in the amount of aluminium, as expected.

This method also highlights the intensity of each compound in each particle (marked in Figure 4-18 to Figure 4-20 according to the sample) as shown in Figure 4-21 to Figure 4-23. As expected, the carbon signal is maintained approximately constant and represents the thin carbon coating and the carbonate ion (CO_3^{2-}); the oxygen signal is quite intense due to its presence in the alumina compound (Al_2O_3) and carbonate ion; however, the sodium and aluminium presences in the samples are not homogeneous, i.e., there are some particles that are mostly made of alumina (spectrum 8, 5 and 11 according to the sample N10, N20 and N40 respectively), some others are just made of sodium carbonate (spectrum 2 and 5 for the samples N20 and N40, respectively) and there are some particles with sodium carbonate dispersed in the alumina surface approximately according to the average percentage of reagents used in each sample (spectrum 5, 9 and 8 for the samples N10, N20 and N40, respectively).

The sum of elements intensity for each sample, represents, as expected, an increase in the amount of sodium and a decrease in the amount of aluminium from the sample N10 to N40.

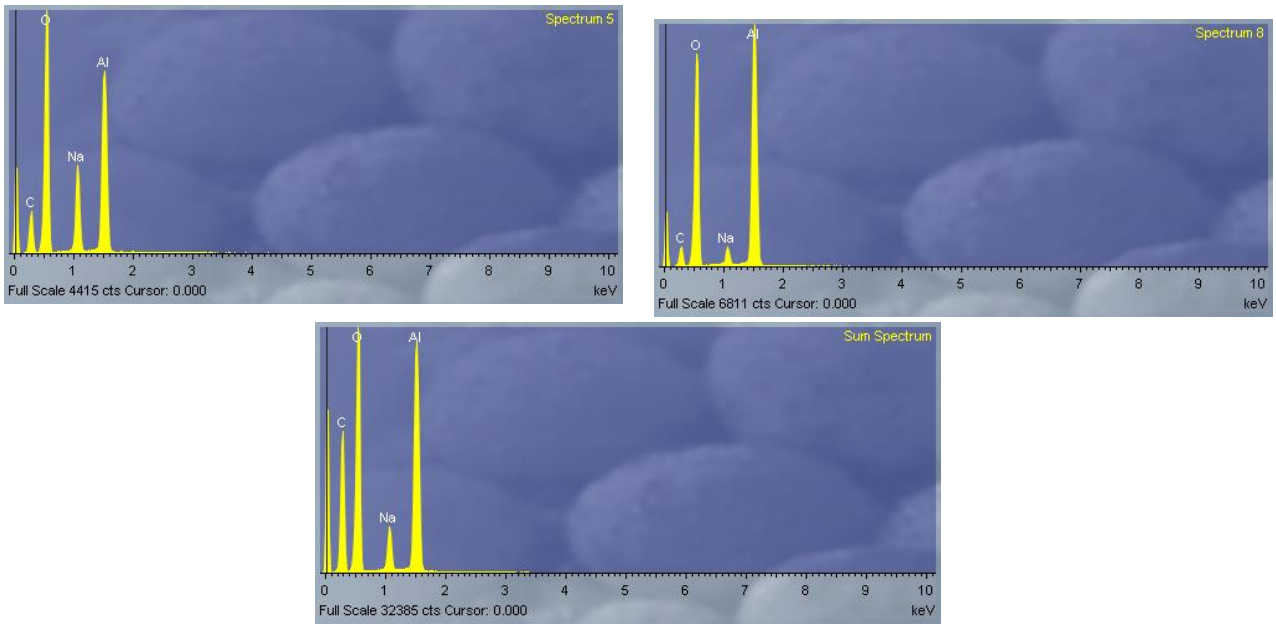

Figure 4-21 – N10 Elements intensity of particles 5 and 8 as well as the sum spectrum with the average element intensity, respectively generated by the INCA-Mapping software.

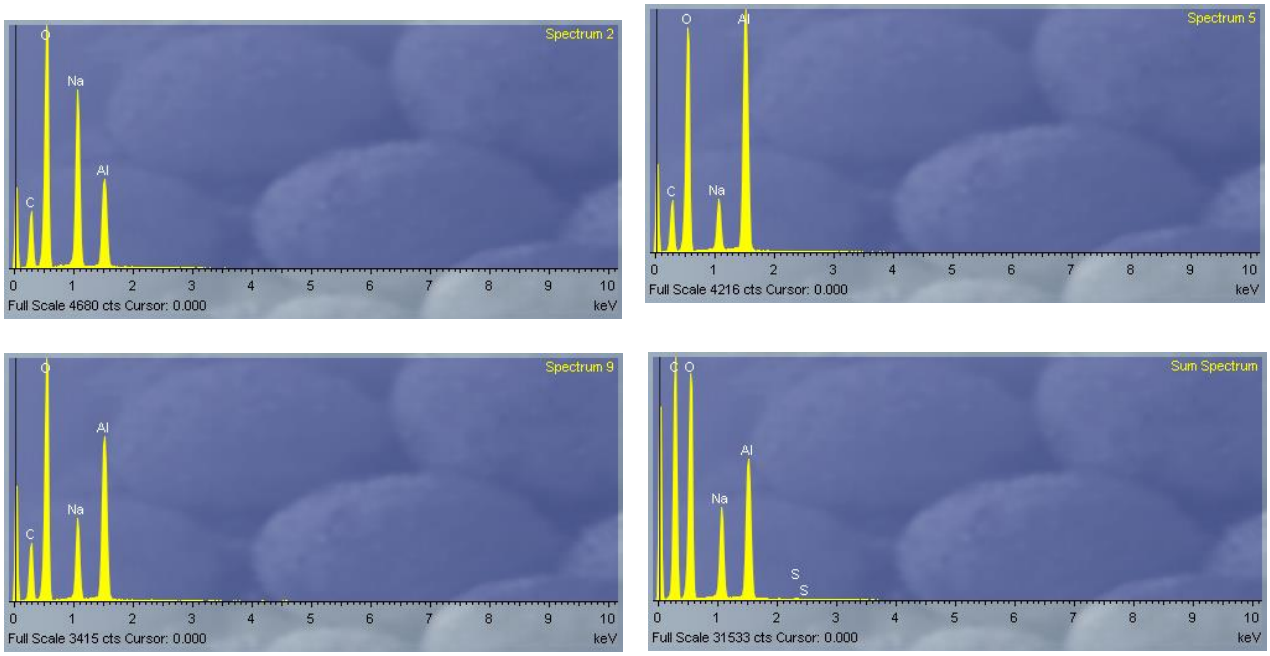

Figure 4-22 – N20 Elements intensity of particles 2, 5 and 9 as well as the sum spectrum with the average element intensity, respectively generated by the INCA-Mapping software.

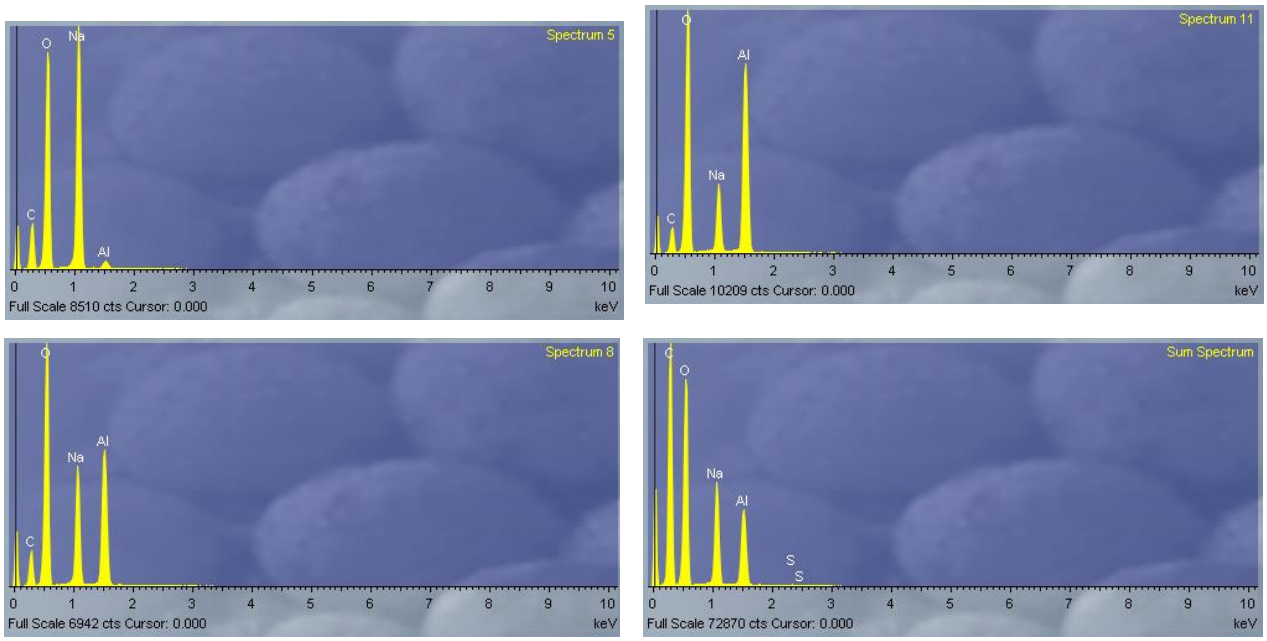

Figure 4-23 – N40 Elements intensity of particles 11, 5 and 8 as well as the sum spectrum with the average element intensity, respectively generated by the INCA-Mapping software.

It was then concluded that there is not homogeneity in each sample, i.e., for each one there are some particles just made with alumina, others just made with sodium carbonate and there are some particles that really have the sodium carbonate disperse in alumina surface. Between the samples and as expected, it was observed that the average of sodium amount increased from N10 to N40 measurements, as well as the aluminium decreased. It was expected that the 0.4 for ration between sodium and aluminium amount, however it was observed that the average amount of sodium is bigger than the aluminium amount. This leads to the conclusion that it is not possible to make inferences about all the sodium-based sorbent prepared due to their heterogeneity.

In order to determine the samples surface area, it was conducted an isotherm measurement with N_2 at 77 K on BELSORP-mini II equipment. The measured samples were previously activated on BELPREP-vacII equipment, with the aim of dehydrate it. Since that previously, the sample was drying on the oven at 90 °C, the activation was performed at 60 °C for 18 h. The adsorption/desorption isotherm results for N10, N20 and N40 samples are plotted in Figure 4-24. The isotherm points at low relative pressure of each adsorption result (before the Inflexion point) are represented in Figure 4-25 as well as the its trend lines according to equation 3-1.

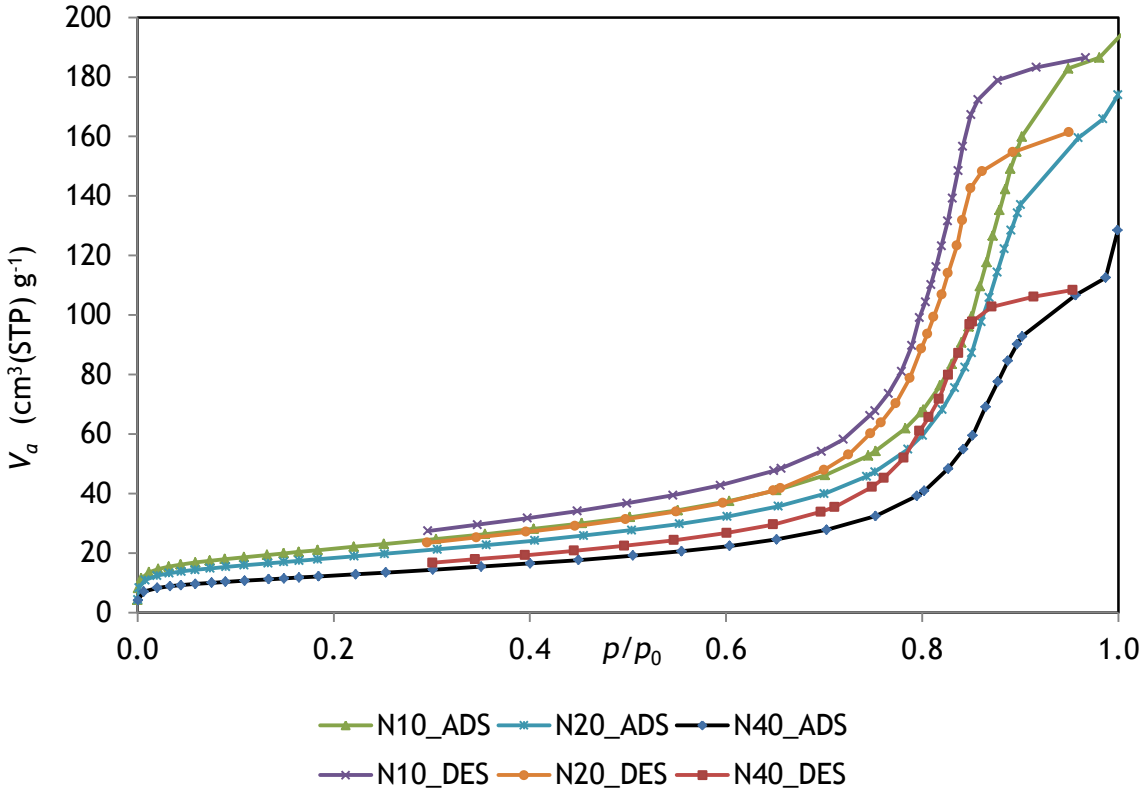

Figure 4-24 - Adsorption/desorption isotherms for N10, N20 and N40 samples, performed with N_2 at 77 K.

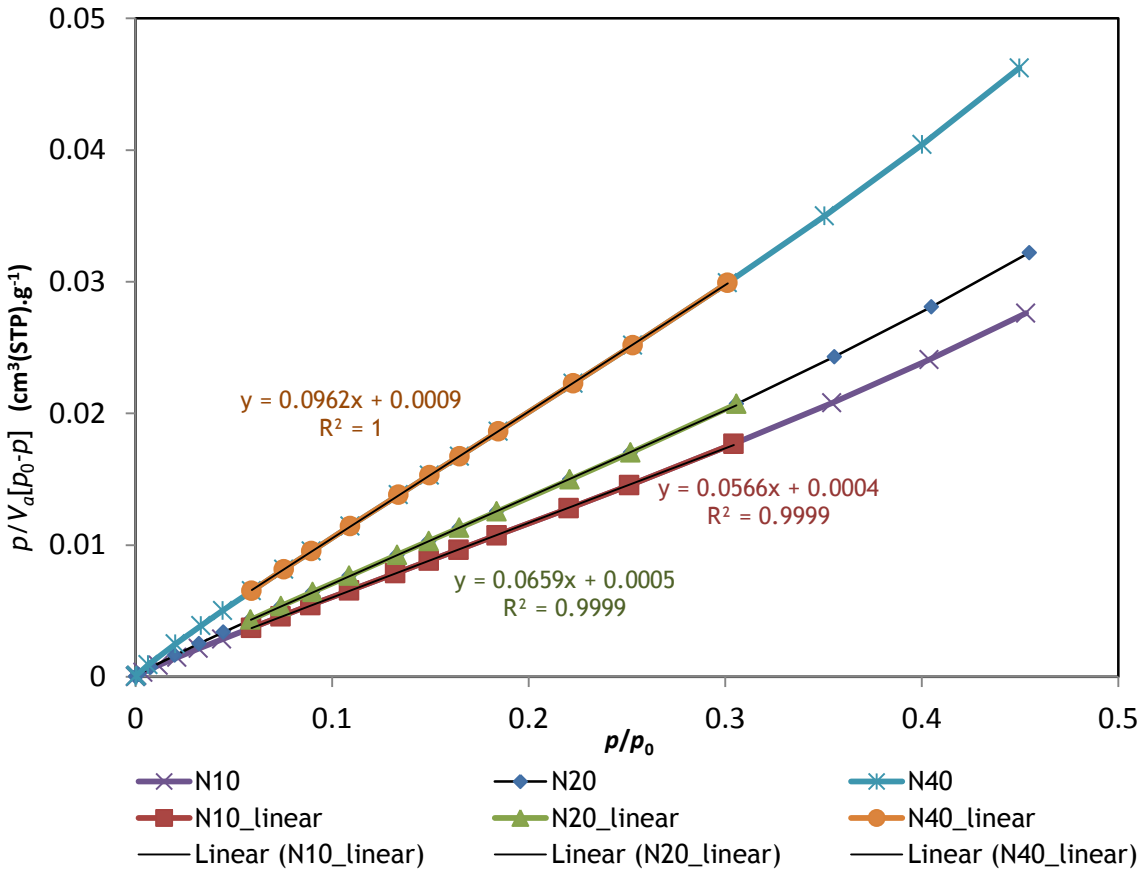

Figure 4-25 - BET plot for N10, N20 and N40 samples performed with N_2 at 77 K.

The surface area value determined by BET method (equation 3-2) is presented in Table 4-2 as well as the intermediary values – V_m and C.

Table 4-2 – BET results for the three carbonate samples

Na_2CO_3	$m_{anlysis}$ (g)	V_m (cm^3(STP)/g)	C	S_{BET} (m^2/g)
10 wt.%	0.12	17.55	152.79	45
20 wt.%	0.11	15.06	141.20	65
40 wt.%	0.10	10.30	108.22	76

The carbonates surface area increased with the amount of sodium carbonate. However, the volume of gas adsorbed at STP to produce an apparent monolayer on the sample surface (V_m) decreased.

In order to test the samples performance, it was measured a breakthrough curve in a column (Figure 3-7) which outlet was connected to a MS analyser as represented in Figure 3-5.

A program was run on BIGCCS software (Figure 3-6) considering a flow rate of 50 mL/min, starting with just nitrogen (N_2) as a feed gas and increasing the temperature until 178 °C for 180 minutes (heating rate of 5 °C/min) in order to activate the particles, i.e., to release all the water and carbon dioxide that could have been taken on the production and storage. After, the system was cooled down to 75 °C and stabilized for 30 minutes. Then the reactor's feed was changed to the *Mix(CO_2)* with humidity, at the same flow rate of 50 mL/min for 200 minutes, corresponding to the adsorption step (equation 2-2) Then, the sample was regenerated again at 178 °C for 180 minutes with a heating rate of 5 °C/min (equation 2-3) and it was started a new cycle. The measured results for samples N10, N20 and N40 are shown in Figure 4-29 to Figure 4-28.

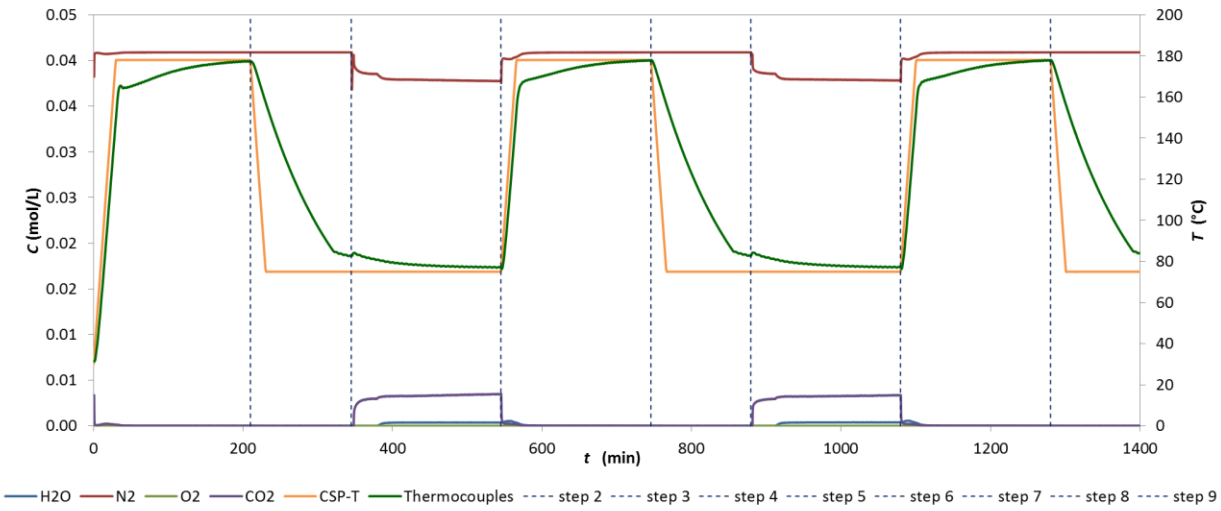

Figure 4-26 - Gas concentration at the exit of the column for sample N10 (H_2O: blue, N_2: red, O_2: light-green and CO_2: purple) as well as the current set point of the oven's temperature (orange line) and measured temperature on thermocouples inside of the column (dark-green) according to the programmable steps (dashed line).

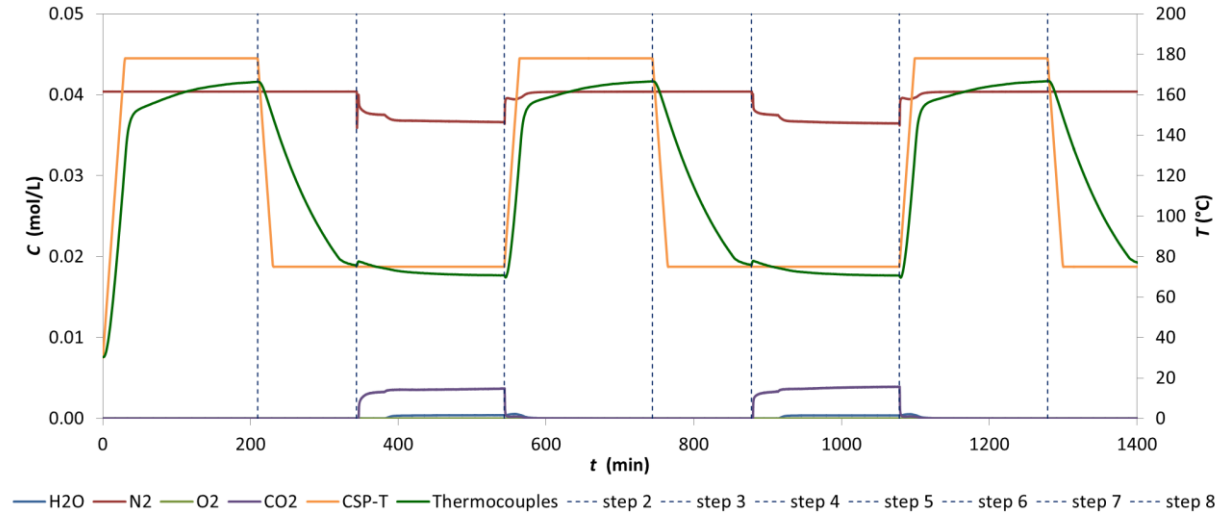

Figure 4-27 - Gas concentration at the exit of the column for sample N20 (H_2O: blue, N_2: red, O_2: light-green and CO_2: purple) as well as the current set point of the oven's temperature (orange line) and measured temperature on thermocouples inside of the column (dark-green) according to the programmable steps (dashed line).

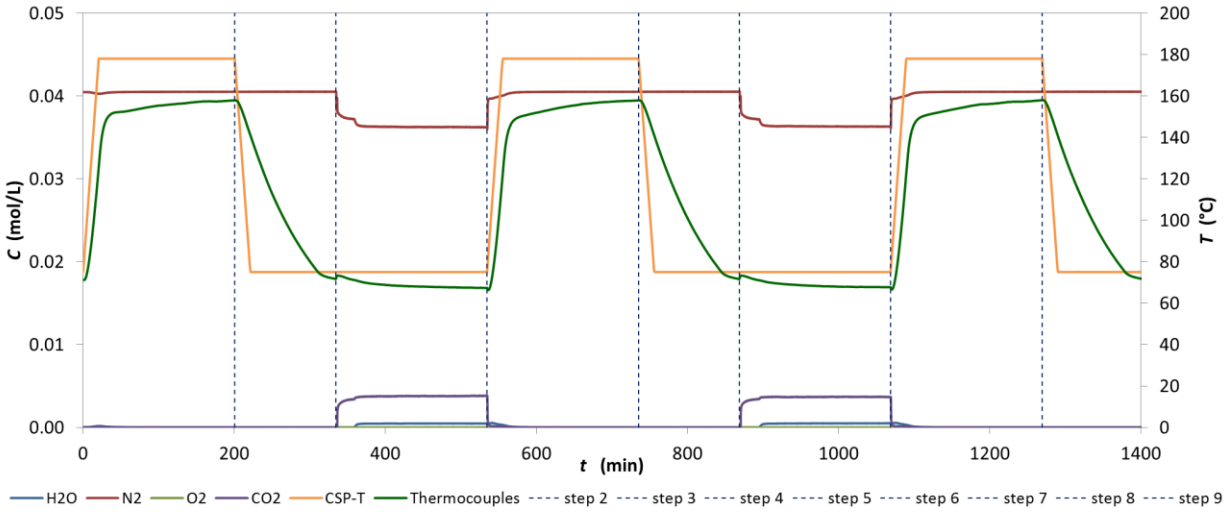

Figure 4-28 - Gas concentration at the exit of the column for sample N40 (H_2O: blue, N_2: red, O_2: light-green and CO_2: purple) as well as the current set point of the oven's temperature (orange line) and measured temperature on thermocouples inside of the column (dark-green) according to the programmable steps (dashed line).

The gas concentration at the exit of the column was calculated through equations 3-3 to 3-7.

Considering that the gas mixture (N_2/O_2) can be approximated to air, the percentage of water on the gas mixture at the entrance of the column (y_{0,H_2O}) was calculated through the determination of the saturation pressure of water vapour at its temperature (11.8 °C) as shown in the following equations.

$$P_{WS} = exp\left(A + B \times T - \frac{E}{T}\right)/T^F \tag{4-1}$$

$$y_{0,H_2O} = \frac{P_{WS}}{P} \tag{4-2}$$

In which P_{WS} is the saturation pressure of water vapour (Pa); A, B, E and F are constants associated to this equation (77.3450, 0.0057, 7235 and 8.2 respectively); T is the temperature of the air vapour mixture (K) [14].

The instrument was not calibrated for the gas mixture, thus the percentage of gas had to be adjusted through interpolation according to the expected values: 9.77 % of CO_2 and 1.43 % of H_2O in a N_2 environment.

The breakthrough results in molar concentration ratio (C/C_0) for the first cycle of N10, N20 and N40 samples are shown in Figure 4-29 to Figure 4-31 as well as the corresponding current

set point of the oven (*CSP-T*) and average of the temperature measured on the thermocouples (Thermocouples), in function of the time divided in steps.

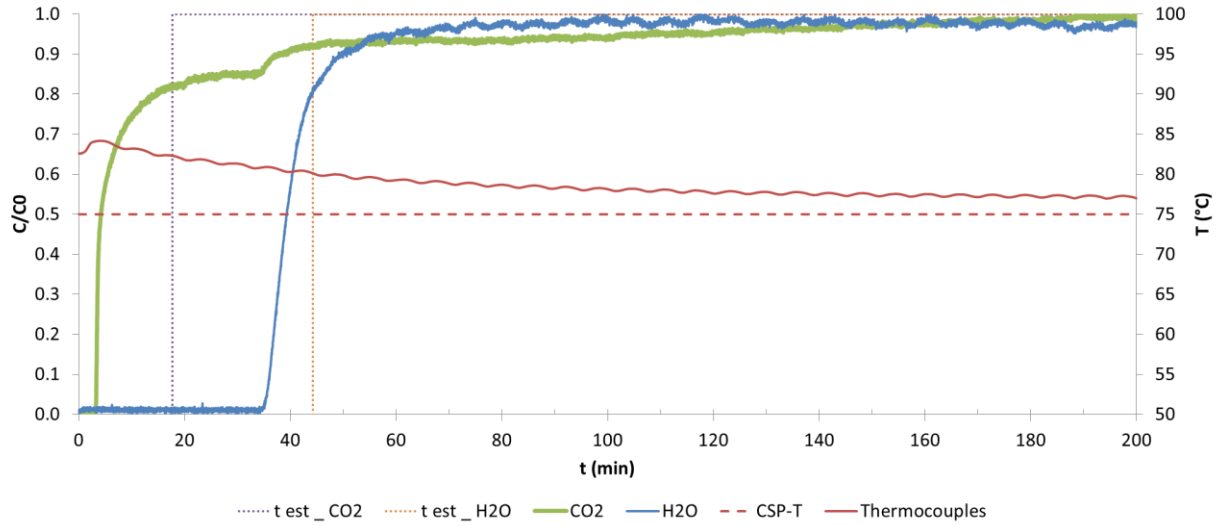

Figure 4-29 - Breakthrough curve of CO_2 and H_2O for N10 sample and respective stoichiometric time as well as the current set point of oven temperature (CSP-T) and average temperature measured in thermocouples inside of the column (Thermocouples)

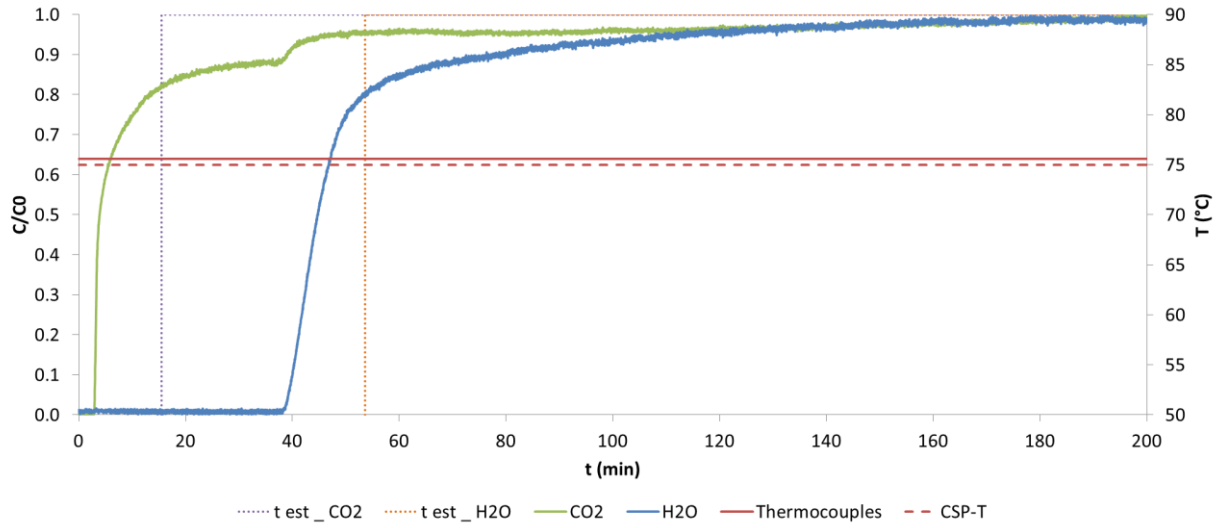

Figure 4-30 - Breakthrough curve of CO_2 and H_2O for N20 sample and respective stoichiometric time as well as the current set point of oven temperature (CSP-T) and average temperature measured in thermocouples inside of the column (Thermocouples)

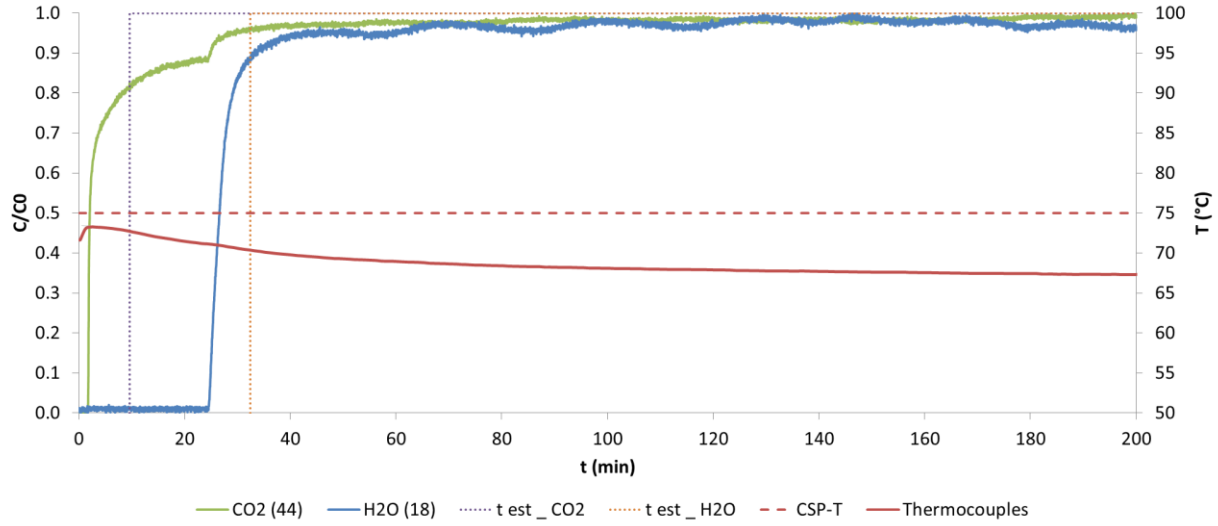

Figure 4-31 - Breakthrough curve of CO_2 and H_2O for N40 sample and respective stoichiometric time as well as the current set point of oven temperature (CSP-T) and average temperature measured in thermocouples inside of the column (Thermocouples)

The CO_2 curve makes a first step and after the water signal starts to appear, the normalized concentration of CO_2 increases again. The feed ratio between the CO_2 and H_2O is around 6.8, which means more amount of CO_2. According to equation 2-2, the adsorption reaction requires one molecule of CO_2 and one molecule of H_2O for one molecule of sodium carbonate. Thus, it is possible to suppose that the first step represents the exceeded CO_2 that can also adsorb at the beginning, and the second step that appears at the same time as the water, represents the CO_2 that was adsorb due to the adsorption reaction (equation 2-2) and to the changes that H_2O could cause in the particle surface.

The initial adsorbent weigh placed in the column and the feed concentrations of CO_2 and H_2O to the column are presented in Table 4-3. The adsorption results for CO_2 and H_2O determined by equations 3-8 and 3-9, are represented in Table 4-4 and Table 4-5.

Table 4-3 - Initial conditions for the breakthrough curve measurements.

	$m_{adsorbent}$ (g)	C_t (mol/L)	CO_2		H_2O	
			y_{CO2}	C_0 (mol/L)	y_{H2O}	C_0 (mol/L)
N10	2.916	0.04	0.098	3.89×10^{-3}	0.014	5.67×10^{-4}
N20	2.834					
N40	2.616					

Table 4-4 – CO_2 adsorption/desorption results for 2 cycles of each SBSSA samples.

	1th cycle			2th cycle		
	Adsorption		Dessorption	Adsorption		Dessorption
	t_{est} (min)	q_{total} (mol_{CO2} /$kg_{adsorvent}$)	q_{total} (mol_{CO2} /$kg_{adsorvent}$)	t_{est} (min)	q_{total} (mol_{CO2} /$kg_{adsorvent}$)	q_{total} (mol_{CO2} /$kg_{adsorvent}$)
N10	17.7	1.18	0.21	13.3	0.89	0.20
N20	15.5	1.07	0.62	16.2	1.12	0.59
N40	9.7	0.72	0.17	5.2	0.39	0.18

Table 4-5 – H_2O adsorption/desorption results for 2 cycles of each SBSSA samples.

	1th cycle			2th cycle		
	Adsorption		Dessorption	Adsorption		Dessorption
	t_{est} (min)	q_{total} (mol_{H2O} /$kg_{adsorvent}$)	q_{total} (mol_{H2O} /$kg_{adsorvent}$)	t_{est} (min)	q_{total} (mol_{H2O} /$kg_{adsorvent}$)	q_{total} (mol_{H2O} /$kg_{adsorvent}$)
N10	44.3	0.43	0.25	43.2	0.42	0.24
N20	53.6	0.54	0.31	45.6	0.46	0.31
N40	32.5	0.35	0.27	37.0	0.40	0.04

The CO_2 capacity of the sample is inversely proportional to the sodium carbonate weight in the sample. However the water capacity increases from N10 to N20 sample and decreases from N20 to N40. It was also noticed that the desorption amount is smaller than the adsorbed for all samples and both gases. However, on the second cycle the sample is able to adsorb more amount then the one that desorbed but less than the one that adsorb on the first cycle.

5 Conclusions

Controlling CO_2 emissions has been a global concern due to its effect as a GHG on the global warming effect. In this sense, the objective of this thesis has focused on the development of two very different porous adsorbents aiming to separate carbon dioxide from very different streams emitters of CO_2 – Mesh-adjustable molecular sieves (MAMS) and Sodium-based sorbent supported in alumina (SBSSA).

MAMS [1] enables the carbon dioxide adsorption at low temperature, being promising due to its selective removal of carbon dioxide in the natural gas industry, particularly when the final product is liquefied natural gas (LNG). On this thesis it was tried to reproduce the experimental procedure reported for MAMS-1 [1], testing also the influence of some production variables.

The samples I1 and I3 were selected as best ones considering the reported features. Still, it was encountered some difficulties in reproducing them with the same reported performance and in larger production amounts (0.2 g/batch). However, one of the authors of the original article describing this adsorbent upon being contacted by e-mail contact responded, "I encountered some difficulties to scale-up to larger than even 0.1 g/batch (…) I used multi-autoclaves to scale it up".

SBSSA, aimed to capture carbon dioxide at milder temperatures (75 °C) that is closer to the temperature of the flue gases emitted in power stations (90 °C in natural gas combined cycles power plants and 110 °C in coal-fired power plants).

3 samples of SBSSA were prepared changing the sodium carbonate weight fraction: 10 wt.% (N10), 20 wt.% (N20) and 40 wt.% (N40). It was found that the particles are not completely homogeneous concerning sodium carbonate layer thickness. The breakthrough curve tests showed that as expected the water has an impact on the CO_2 capture. However, it would be necessary to run more tests in order to understand what really happens on the particles during long lasting adsorption/desorption experiments.

5.1. Goals Achieved

The MAMS production tests showed that as expected from the article's authors [1], it is not possible to "scale it up". However, even the samples produced in small amounts but still more than the amount produced by the authors, do not have capabilities to adsorb carbon dioxide.

The SBSSA production method conducted didn't have good results in homogeneity. Still, it was observed that at 70 °C the particles are able to adsorb carbon dioxide. However it would be necessary to run some more tests to observe the durability of the material.

5.2. Limitations and Future Work

During this internship it was possible to learn not only in a scientific level but also how the work in real life carried out. In research it is not easy to make some trials and run some tests whenever possible. Thus, some parts of the work has to be stopped for some time waiting for available equipment or even to make decisions about the next step.

Nevertheless, it was possible to perform several experiments and characterization tests on both types of solid sorbents (MAMS and SBSSA). However, some more tests would be necessary to run for a better understanding of particles behaviour.

MAMS project ended with these results while the research work carried out in SBSSA will be continued by Sorbent Technologies department on SINTEF.

6 References

[1] Shengqian Ma; Daofeng Sun; Xi-Sen Wang; Hong-Cai Zhou. *A Mesh-Adjustable Molecular Sieve for General Use in Gas Separation*. Angew. Chem. Int. Ed. 2007, 46, 2458 – 2462.

[2] Matthew E. Boot-Handford; Juan C. Abanades; Edward J. Anthony; Martin J. Blunt; Stefano Brandani; Niall Mac Dowell; José R. Fernandez; Maria-Chiara Ferrari; Robert Gross; Jason P. Hallett; R. Stuart Haszeldine; Philip Heptonstall; Anders Lyngfelt; Zen Makuch; Enzo Mangano; Richard T. J. Porter; Mohamed Pourkashanian; Gary T. Rochelle; Nilay Shah; Joseph G. Yao; Paul S. Fennell. *Carbon Capture and Storage Update*. Energy Environ. Sci. DOI: 10.1039/c3ee42350f.

[3] Zongbi Bao; Sufian Alnemrat; Liang Yu; Igor Vasiliev; Qilong Ren; Xiuyang Lu; Shuguang Deng. *Kinetic separation of carbon dioxide and methane on a copper metal-organic framework*. Journal of Colloid and Interface Science. DOI: 10.1016/j.jcis.2011.01.103.

[4] *MOF Scheme*. [image] Available at: http://cdn.phys.org/newman/gfx/news/201029press.gif Accessed 2014/6.

[5] Ya Liang. *Carbon Dioxide Capture From Flue Gas Using Regenerable Sodium-Based Sorbents*. M. S. Thesis. Lousiana State University. August 2003. [online] http://etd.lsu.edu/docs/available/etd-0702103-151700/unrestricted/Liang_thesis.pdf. Accessed 2014/5.

[6] Ya Liang; D. P. Harrison; R. P. Gupta; D. A. Green; W. J. McMichael. *Carbon Dioxide Capture Using Dry Sodium-Based Sorbents*. Energy & Fuels. 2004. 18 (2). 569-575.

[7] IEA Greenhouse Gas R&D Programme (IEA GHG). *Post combustion carbon capture from coal fired plants – solid sorbents and membranes*. 2009/2. [online] http://decarboni.se/sites/default/files/publications/98346/post-combustion-carbon-capture-coal-fired-plants-solid-sorbents-membranes.pdf. Accessed 2014/5.

[8] Martin Ermrich; Detlef Opper. *X-Ray Powder Diffraction*. PANalytical GmbH. 2011.

[9] John Goodge. *Back-scattered Electron Detector (BSE)*. University of Minnesota. 2013/6. [online] http://serc.carleton.edu/research_education/geochemsheets/bse.html Accessed 2014/6.

[10] John Goodge. *Energy-Dispersive X-Ray Spectroscopy (EDS)*. University of Minnesota. 2013/12. [online] http://serc.carleton.edu/research_education/geochemsheets/eds.html Accessed 2014/6

[11] *Derivation of the BET and Langmuir Isoterms*. University of Colorado. 2011/11. [online] http://chem.colorado.edu/chem4581_91/images/stories/IsothermDerv.pdf. Accessed 2014/5

[12] Nina Hwang; Andrew R. Barron. *BET Surface Area Analysis of Nanoparticles*. 2011. [online] http://cnx.org/content/m38278/latest/. Accessed 2014/5.

[13] Shengqian Ma; Daofeng Sun; Xi-Sen Wang; Hong-cai Zhou. *A Mesh-Adjustable Molecular Sieve (MAMS) Omnipotent in Gas Separation*. Department of Chemistry and Biochemistry, Miami University. 2007.

[14] *Water Vapor and Saturation Pressure in Humid Air*. [online] http://www.engineeringtoolbox.com/water-vapor-saturation-pressure-air-d_689.html. Accessed 2014/4.